



**Yarmouk University**  
**Hijawi Faculty for Engineering Technology**  
**Department of Computer Engineering**

Control of Variable speed drive (VSD) based on Diode clamped  
multilevel inverter using Field oriented control

**M.Sc.Thesis**

**By**

**Laith Quraan**

**Advisor**

**Dr.Ibrahim Al-Tawil**

**Co-advisor**

**Dr.Amin Alqudah**

**June, 2012**

Control of Variable speed drive (VSD) based on Diode clamped  
multilevel inverter using Field oriented control

By

Laith Ghazi Quraan

B. Sc Mechatronics Engineering, Mechatronics Engineering Department,  
Hashemite University, zarqa- Jordan

A thesis Submitted in partial fulfillment of the requirements for the  
degree of Master of Science, in the department of computer Engineering,  
Yarmouk University, Irbid, Jordan

Approved by:

**Dr. Ibrahim Al-Tawil** .....Chairman  
*Associate Professor of Electrical Engineering, Yarmouk University*

**Dr.Amin Alqudah** .....Member  
*Assistance Professor of computer Engineering, Yarmouk University*

**Dr. Mahmood Al-khassaweneh** .....Member  
*Assistance Professor of computer Engineering, Yarmouk University*

**Dr. Shadi Alboon** .....Member  
*Assistance Professor of Electronic Engineering, Yarmouk University*

## ACKNOWLEDGMENTS

*I would like to thank my adviser Dr.Ibrahim Al-Tawil and co-advisor Dr.Amin Alqudah for their assistance, direction and guidance. I also wish to express my deep gratitude to all my family members and my parents, for their support and love.*

# TABLE OF CONTENTS

Abstract.....	I
List of Figures .....	II
List of Tables .....	IV
1. Introduction.....	1
1.1 Background.....	1
1.2 Literature review .....	4
1.3 Objectives of the study and Thesis Organization.....	5
2. Induction motor .....	6
2.1 Introduction.....	6
2.2 Squirrel cage induction motor.....	6
2.3 Principles of operation.....	8
2.4 Parameter of the induction motor .....	10
3. Multilevel inverter .....	11
3.1 Introduction .....	11
3.2 Diode clamped multilevel inverter .....	13
3.3 Modulation techniques .....	16
3.4 Level shifted modulation results .....	20
3.4.1 In-phase disposition.....	20
3.4.2 Alternative phase opposite disposition.....	23
3.4.3 Phase opposite Disposition.....	24

4. Dynamic modeling of induction motor .....	26
4.1 Three phase mathematical modeling of induction motor .....	26
4.2 Space vector definition and projection .....	30
4.2.1 Stationary reference frame ( $\alpha$ - $\beta$ ) .....	31
4.2.2 Rotating reference frame (d-q) .....	34
5. Field Oriented Control and Simulation results .....	38
5.1 Concept of field oriented control .....	38
5.2 Method based of field oriented control .....	39
5.2.1 Indirect field oriented control .....	40
5.2.2 Principle of operations .....	41
5.3 Speed Loop Controller.....	42
5.4 Current Controllers.....	43
5.4.1 Hysteresis Controller .....	43
5.4.2 Stator frame PI controllers.....	45
5.4.3 Synchronous - Frame PI Control.....	46
5.5 Simulation results .....	47
6. Conclusion and future work .....	53
6.1 Conclusion.....	53
6.2 Future work.....	54

7. References .....	55
8. Appendixes.....	60

© Arabic Digital Library-Yarmouk University

## DECLARATION

---

I am, **Laith Ghazi Quraan**, recognize what plagiarism is and I hereby declare that this thesis proposal, which is submitted to the department of computer Engineering at Hijjawi Faculty for Engineering Technology, for the partial fulfillment of the requirements for the degree of Master of Science, is my own work. I have not plagiarized from any sources. All references and acknowledgments of sources are given and cited in my proposal. I have used the conventional citation and referencing. Each significant contribution to and quotation in this report from work of other people has been attributed and referenced.

Laith Quraan

June, 2012

## **Abstract:**

This thesis presents the simulation of an Indirect Field Oriented Control for Variable speed drives (VSD) feed by multilevel inverter. A diode clamped multilevel inverter and an induction machine will be used as prototypes. The indirect rotor-flux-oriented control of the induction machine supplied by a 7-level diode clamped voltage-source inverter with fast Synchronous Frame proportional-integral (PI) current control is employed; the magnitude and space angle of the rotor flux linkage is obtained by d-q model. The level shifted carriers-base pulse width modulation (PWM) techniques will be used to control of the multilevel inverter. The simulation used to identify the performance of indirect field oriented control in terms of speed, torque, current ripple and transient response. The MATLAB/SIMULINK will be used as simulation tool in this work.

**Keywords:** Diode -Clamped Multilevel Inverter, Indirect Field-oriented control (IFOC), Induction motor, carriers-base pulse width modulation (PWM).



## LIST OF FIGURES

Fig.1.1 General Classification of induction motor control methods.....	2
Fig2.1 three phase induction motor .....	7
Fig 3.1 seven level diode clamped inverter .....	13
Fig 3.2 modulation techniques for multilevel inverter .....	16
Fig 3.3 In-phase disposition (IPD) .....	17
Fig 3.4 Alternative phase opposite disposition (APOD) .....	18
Fig 3.5 Phase opposite disposition (POD) .....	18
Fig 3.6 Logic to generate gating signals for IGBTs in matlab simulink. ....	19
Fig 3.7 output phase voltage of 7-level diode clamped inverter based on In-phase disposition (IPD) level shifted modulation .....	21
Fig 3.8 output line-line voltage of 7-level diode clamped inverter based on In-phase (IPD)...	21
Fig 3.9 Harmonic spectrum of phase voltage based on In-phase disposition (IPD).....	22
Fig 3.10 Harmonic spectrum of line to line voltage based on (IPD).....	22
Fig 3.11 Harmonic spectrum of phase voltage Based on alternative phase opposite disposition (APOD).....	23
Fig 3.12 Harmonic spectrum of line-line voltage Based on (APOD).....	23
Fig 3.13 Harmonic spectrum of line-line voltage based on phase opposite disposition (POD).....	24
Fig 3.14 Harmonic spectrum of phase voltage based on (POD).....	24
Fig4.1 Equivalent Circuit of an AC Induction Motor.....	27
Fig 4.2 Stator current space vector .....	31

Fig 4.3 Stator Current Space Vector and Its Projection.....	32
Fig 4.4 general reference frame rotates at a general speed $\omega_g$ .....	34
Fig 4.5 dynamic d-q equivalent circuit (a) q-axis and (b) d-axis .....	37
Fig 5.1 rotor flux oriented control. ....	39
Fig 5.2 indirect field oriented control .....	41
Fig 5.3 Step response of speed controller .....	42
Fig 5.4 principle of hysteresis control .....	44
Fig 5.5 scheme of hysteresis current control .....	45
Fig 5.6 Stator frame PI controllers .....	46
Fig 5.7 Synchronous - Frame PI Control .....	46
Fig 5.8 speed response .....	47
Fig 5.9 Speed variation at $t=1$ s when a load of 45Nm is connected. ....	48
Fig 5.10 Torque response .....	49
Fig 5.11 three phase Stator currents .....	49
Fig 5.12 Line-line voltage waveform .....	50
Fig 5.13 Line-line voltage waveform in steady state .....	50
Fig 5.14 Harmonic spectrum of line-line voltages of a phase A .....	51

## List of Tables

Table 2.1 Parameters of the induction motor .....	10
Table 3.1 Diode-clamped 7-level inverter voltage levels and corresponding switch states...14	
Table 3.2 Parameters used for level shifted modulation technique .....	20
Table 3.3 Level shifted modulation results.....	25
Table 5.1 Response of the system with different values loads.....	51

## Chapter 1: INTRODUCTION

### 1.1 Background

A Variable Speed Drives (VSD), also known as Variable Frequency Drives (VFD), have gained much attention in the industrial applications, where high reliability is required. A key concern of VSD is to provide energy saving and to increase productivity in many industrial applications such as pumps, fans, elevators, electrical vehicles, heating ventilation and air-conditioning (HVAC), robotics, wind generation systems, ship propulsion, etc[1], [2] and [3].

Squirrel Cage Induction Motors (IM) and Permanent Magnet Synchronous Motors (PMSM) are the most used in those drives [3].

In the past, DC (Direct Current motors) machines were preferred for variable speed drives. However, DC motors have many drawbacks such as high cost, high rotor inertia and maintenance problem with commutators and brushes. In addition they cannot operate in dirty and explosive environments. The AC (Alternating Current motors) machines do not have the drawbacks of DC machines. Therefore, in last three decades the inverter-fed AC motor has largely taken place in variable speed applications, where the DC motors are increasingly replaced by AC drives [4] and [5]. The reason for those results is development of Digital Signal Processor (DSP) technologies and modern semiconductor devices.

Multilevel inverters are being increasingly used in high power industrial applications because it gives good power quality, high voltage capability, low switching losses and good electromagnetic compatibility (EMC) [6] and [10]. For the outside applications where cabling the AC power for the desired location is impossible where constant or variable speed drive

system is needed, the multilevel inverter gives the suitable solution. With more levels the output waveform of the inverter is much closer to the sinusoidal waveform.

Control of VSD fed by multilevel inverter has been adapted in many researches paper recently [2], [10], [7] and [9]. A general classification of the variable speed IM control methods is presented in Fig 1.1. These methods can be divided into two groups: scalar and vector.

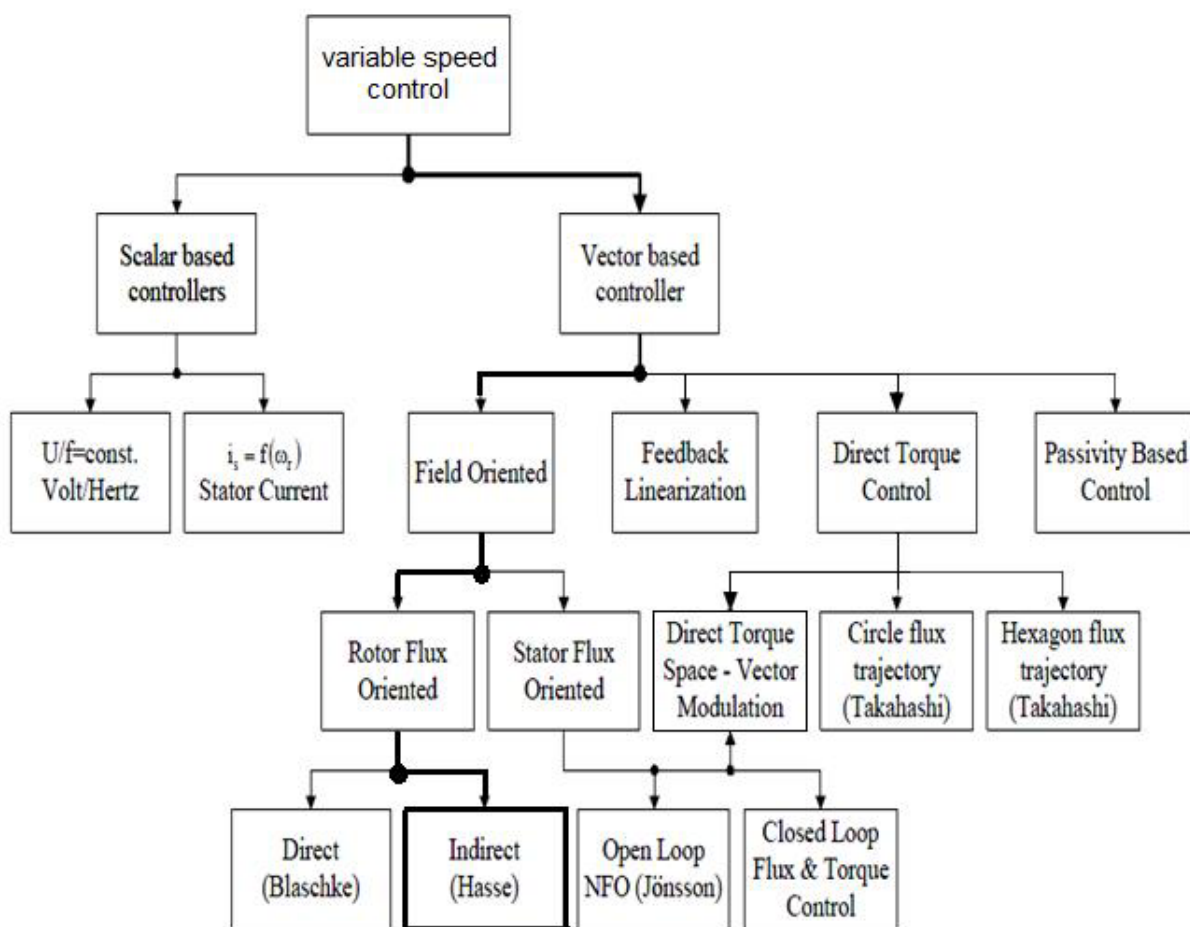


Fig 1.1 General Classifications of Induction Motor Control Methods

The scalar control methods are one of the most popular methods to control of the inverter fed IM in low performance industrial applications [8]. In these methods, which are based on relationships valid in steady state, only the magnitude and the frequency (angular speed) of

voltage, current, and flux linkage space vectors are controlled. Scalar controlled drives give somewhat low performance response, but they are easy to implement [11]. In other hand, in the vector control, which is based on relations valid for dynamic states, the instantaneous positions as well as the magnitude and frequency of voltage, current, and flux linkage space vectors are controlled, what further significantly improve dynamic behavior of the system. The vector control method can be implemented in several ways based on different ideas and analysis.

The first vector control method of induction motor was Field Oriented Control (FOC) presented by F. Blaschke in early of 70s [11]. FOC of Induction motor fed by multilevel inverter has been adapted in many researches paper recently [9] and [7]. The main idea of field orientation control is to achieve decoupled control over the torque and flux producing components of the stator currents like in separately excited dc machine; this is done by transform a three phase stator current into two phase coordinate system rotating with the angular speed equal to rotor flux angular speed.

Another method is Direct Torque and Flux Control (DTFC), also known as Direct Torque Control (DTC), has been developed by I. Takahashi in the middle of 80s. Recently, it has provided an industrial alternative to the field oriented control strategy [11] and [12]. This strategy proposed to replace current regulation loops, like in FOC, by hysteresis controllers, which corresponds to generate gate drive pulses for the inverter semiconductor power devices.

## 1.2 Literature review:

Several research papers studied control of variable speed drive (VSD) targeting better results relevant to which are listed in the references page as follows:

1. In [21] the work dealt with analyses of the control for a subsea drive with multilevel inverter (MLI), it developed a general model for analyzing a variable speed drive with a MLI, the research adapt a three phase cascaded H bridge MLI fed to induction motor, the research adapt Field Oriented Control and Direct Torque Control as a Control Strategies of Induction Motor Drives.
2. Another researcher used numerical simulation to show that the 2-level and 3-level inverter have the same dynamic performance with lower torque and flux ripples as well as lower harmonic content for 3-level inverter by applying the Direct torque control (DTC) in induction motor electrical drive supplied by 3-level diode clamped inverters [32] .
3. Comparative study has been presented in [33] between field oriented control and direct torque control for Permanent Magnet Synchronous Motor (PMSM). The comparison was based on dynamic performance and implementation complexity.
4. A new method has been used in [14], estimating the speed of the induction motor with observer laid in dq-axis, proposing actual motor model using Alfa- Beta axis is what would be usually used, however, the observer used the motor models in rotor flux oriented control (RFOC).

### 1.3 Objectives of the study and Thesis Organization

The objectives of this work are to review the theoretical basis and simulation of control variable speed drive (VSD) based on diode clamped multilevel inverter using field oriented controller. MATLAB/SIMULINK software will be used in this work. The objectives are as follows:

- 1- A 7-level diode clamped inverter will be designed and tested.
- 2- A three phase squirrel cage induction motor will be considered and investigated to be used as prototype.
- 3- Design and utilize the field oriented control as a controller in this work.
- 4- The performance of the control scheme will be tested in terms of torque, speed and current ripple, and transient response to step variations of the command.
- 5- Examining the performance of the complete system with different values of induction motor loads.

This thesis is arranged as follows; Chapter two discusses the construction of three phase squirrel cage induction motor. The principal of operation of the induction motor is also presented. Chapter three focus on diode clamped multilevel inverter and level shifted multicarrier modulation technique to control of seven level diode clamped inverter. Several mathematical models for three phase squirrel cage induction motor are presented in chapter four. Chapter five discusses the concept of field oriented control and the simulation result.



## Chapter 2: INDUCTION MOTOR

### 2.1 Introduction

An AC induction or asynchronous motor (IM) is a rotating electric machine designed to operate from a 3-phase source of alternating voltage. This motor is the prime mover for the vast majority of machines and processes in many industrial applications such as driving pumps, fans, compressors, mixers, mills, conveyors, crushers, elevator, electric vehicle, etc. The characteristic features such as simple and rugged construction, Low cost and minimum maintenance, High reliability and sufficiently high efficiency make it a very economically viable choice for industrial applications [14] and [15]. To clearly understand how a vector control system works it is essential to firstly understand the principal operation of the induction motor. This chapter serves as a background to the 3-phase squirrel cage IM as well as an introduction to various methods available to describe the IM.

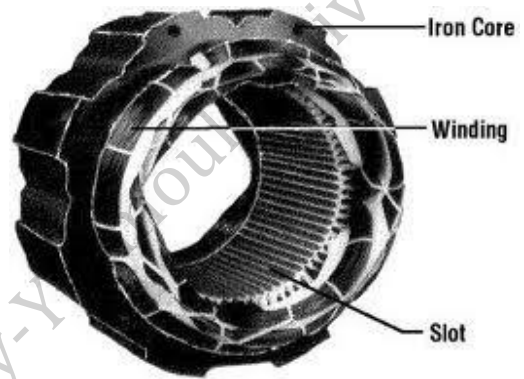
### 2.2 Squirrel cage induction motor

The AC squirrel cage induction motor basically consists of two parts, stator which is stationary and rotor which rotates about the ends supported by bearings as shown in Fig 2.1 (a). The stator is the outer stationary part of the motor, which is consists of a series of wire windings of very low resistance permanently attached to the motor frame as shown in Fig 2.1 (b). As a voltage and a current are applied to the stator winding terminals, a rotating magnetic field is developed in the windings. The stator windings are arranged, the magnetic field appears to synchronously rotate electrically around the inside of the motor housing. The rotor is the rotating part of the motor, which is comprised of a number of thin bars, usually aluminum, mounted in a

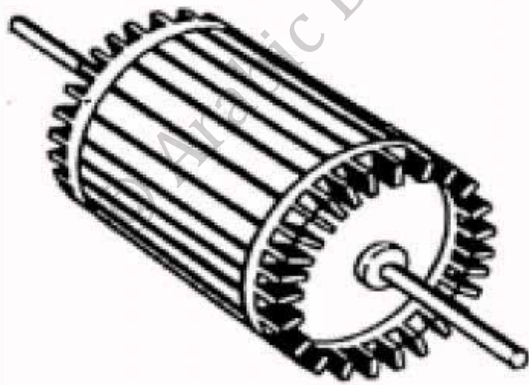
laminated cylinder. The bars are arranged horizontally and almost parallel to the rotor shaft as shown in Fig 2.1 (c). At the ends of the rotor, the bars are connected together with a “shorting ring”. The rotor and stator are separated by an air gap which allows free rotation of the rotor.



a) Squirrel Cage Induction Motor [29]



b) Stator structure [30]



c) Rotor structure [31]

Fig 2.1 Three phase induction motor

## 2.3 Principles of operation

The connection of the stator terminals of an AC induction motor to a 3-Phase AC power supply induces a 3-Phase alternating current to flow in the stator windings. Those currents produce a rotating magnetic flux that rotates inside the motor air gap. This speed of rotation in synchronization with the frequency is named the synchronous speed. The synchronous speed is a function of the number of poles of the motor and the supply frequency as shown in the relationship below:

$$N_{syn} = 120 \frac{f}{P} \dots\dots\dots(2.1)$$

Where ,

$N_{syn}$ : Synchronous rotating speed in rev/min.

$f$ : Power supply frequency in hertz.

$P$ : Number of poles.

The rotating magnetic flux, accordance with Faraday's law, generated in the stator induces an electromotive force (EMF) in the rotor bars. In turn, a current is produced in the rotor bars and shorting ring and another magnetic field is induced in the rotor with an opposite polarity of that in the stator. The rotor magnetic field interacts with the rotating stator flux to produce the rotational force and in accordance with Lenz's law the rotor will accelerate to flow in the direction of rotating flux. Practically the rotor speed doesn't reach the synchronous speed [15], speed of stator rotating magnetic flux, due to friction losses and windage (resistance create when the rotor cut the air at a high speed) [15]. However, if the rotor rotates at synchronous speed, then the rotor bars will be stationary relative to the rotating magnetic field and there will be no

induce voltage in the rotor. The IM can thus speed up to near synchronous speed, but it can never exactly reach synchronous speed. The difference between the synchronous speed and the rotor speed knows as slip speed. Typically, the slip is expressed as a percentage of the synchronous speed. The equation for the motor Slip is:

$$N_{slip} = N_{sync} - N_r \dots\dots\dots (2.2)$$

$$\omega_{slip} = \omega_{sync} - \omega_r \dots\dots\dots (2.3)$$

$$S = \frac{N_{slip}}{N_{sync}} \times (100\%) = \frac{\omega_{slip}}{\omega_{syn}} \times (100\%) \dots\dots\dots (2.4)$$

Where ,

$N_{slip}$ : slip speed of the machine in rev/min.

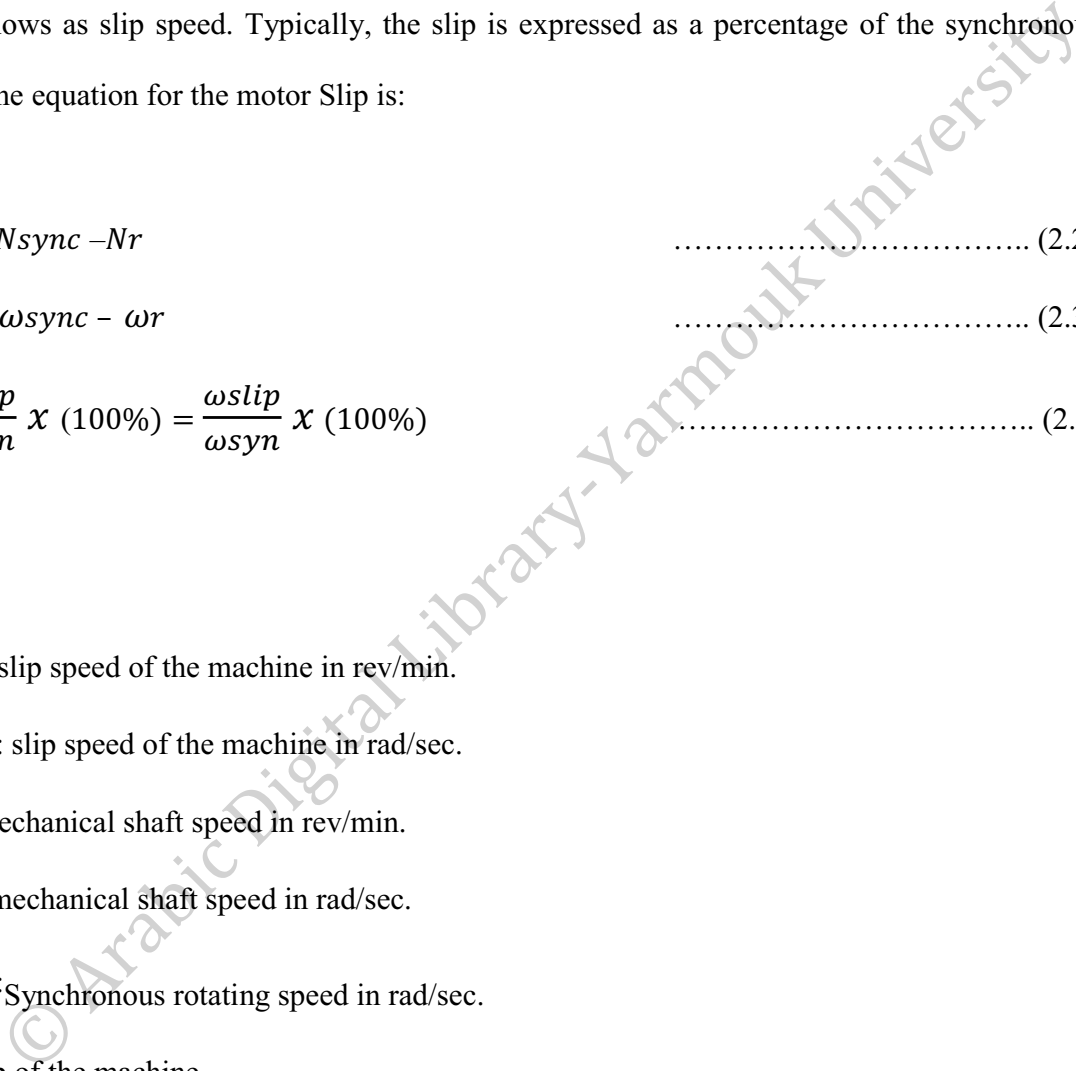
$\omega_{slip}$  : slip speed of the machine in rad/sec.

$N_r$ : mechanical shaft speed in rev/min.

$\omega_r$  : mechanical shaft speed in rad/sec.

$\omega_{slip}$  : Synchronous rotating speed in rad/sec.

S: slip of the machine.



## 2.4 Parameter of the induction motor

In order to investigate of VSD fed by seven levels diode clamped inverter using Field Oriented Control (FOC). A three phase squirrel cage IM was used as prototype. The parameters of the IM are listed in the table below.

Table 2.1 Parameters of the IM

<b>Parameter</b>	<b>Value</b>
Rated output power (kW)	3
Frequency (Hz)	50
Rated voltage (V)	460
Stator winding resistance ( $\Omega$ )	0.294
Stator winding leakage inductance(mH)	1.39
Rotor winding resistance ( $\Omega$ )	0.156
Rotor winding leakage inductance (mH)	0.74
Magnetizing inductance (mH)	41
No of Poles	4
Moment of Inertia (kg m <sup>2</sup> )	0.05

## Chapter 3: Multilevel Inverters

### 3.1 Introduction

A multilevel inverter is a power electronic system that synthesizes a sinusoidal voltage output from several DC sources. These DC sources can be capacitors, batteries, fuel cells, solar cells, etc. The concept of multilevel converters has been introduced as three levels since 1975 by Nabae et al. Subsequently [16], several multilevel converter topologies have been developed. The Multilevel inverters used as the solution to increase the converter operating voltage above the voltage limits of classical semiconductors. The multilevel voltage source inverter is recently applied in many industrial applications such as ac power supplies, static VAR compensators, drive systems, etc [17].

The main idea of multilevel inverters is to have a better sinusoidal voltage and current in the output by using a series of power semiconductor switches with several lower voltage dc sources. With an increasing number of dc voltage sources, the converter output voltage waveform is much closer to the sinusoidal waveform [16], [17] and [18]. The attractive features of a multilevel converter can be summarized as follows:

1. Reduce the  $dv/dt$  stresses on the switching devices due to the small increment in voltage steps.
2. Electromagnetic compatibility (EMC) problems can be reduced when operated at high voltage.
3. Better output voltage quality in term of less distortion, lower harmonics contents and lower switching losses.

4. Reduce the Common-mode (CM) voltage (the average voltage seen at the motor terminals). Therefore, the stress in the motor bearings can be reduced.

Unfortunately, multilevel converters have some disadvantages. One particular disadvantage is the greater number of power semiconductor switches needed. Furthermore each switch requires a related gate drive circuit. This may cause the overall system to be more expensive and complex.

Several multilevel converter topologies have been proposed during the last two decades. At this time, there are three topologies of multilevel inverter, diode-clamped (neutral-clamped) multilevel inverter (DCMLI), cascade H-bridge inverter with separate dc sources and flying capacitor (capacitor clamped) multilevel inverter (FCMLI) [6] and [9]. In DCMLI the dc-link is dividing into number of smaller voltage levels using a bank of series connected capacitors. In FCMLI the capacitor can be kept charged to half the dc-link voltage and the capacitor voltage can be added or subtracted from the dc-link voltage to generate more output levels of the inverter [27]. The concept of cascade H-bridge inverter is based on connecting H-bridge cell in series to get a sinusoidal voltage output. The output voltage is the sum of the voltage that is generated by each cell [28].

This chapter focuses on the main features of multilevel diode clamped inverter, and level shifted carriers-base Pulse Width Modulation (PWM) techniques to control of the multilevel inverter, because it will be use in our work.

### 3.2 Diode-Clamped Multilevel Inverter

Neutral-Point- Clamped multilevel inverter, also known as Diode Clamped multilevel inverter, has gained much attention and widely used in industrial application [19]. This structure was first presented by Nabae *et. al* in 1980 [20]. Fig 3.1 shows one leg of the 7-level NPC inverter.

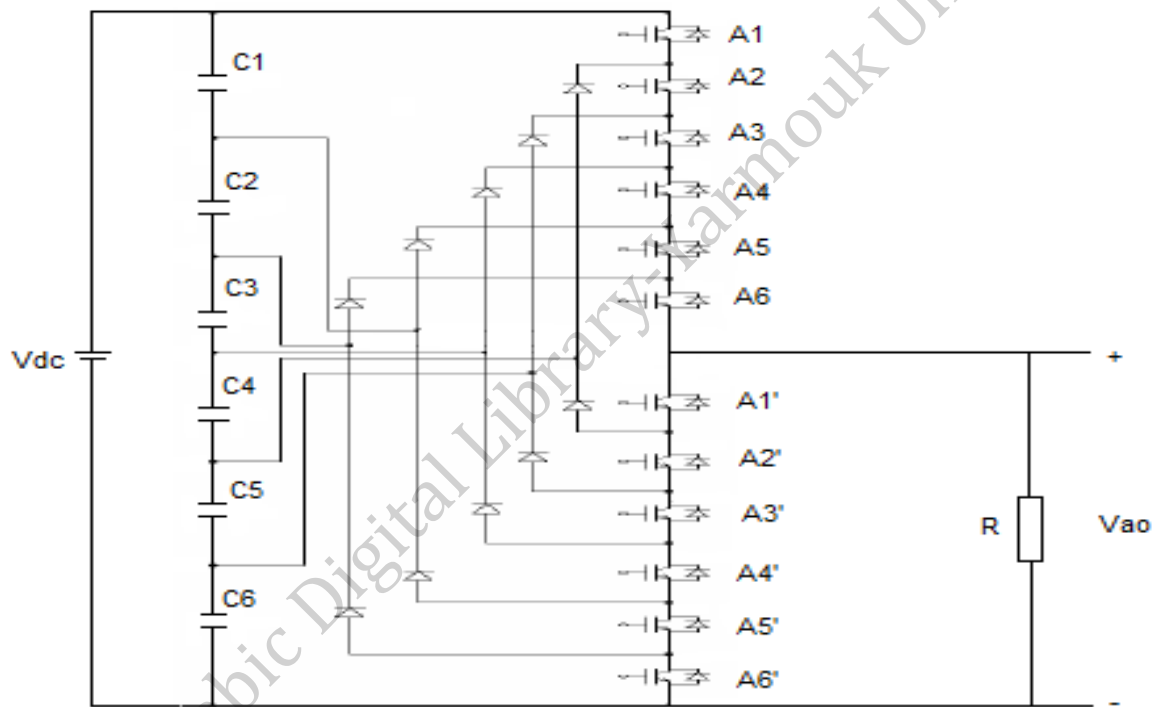


Fig 3.1 Seven Level Diode Clamped Inverter

Each of the three phases of the inverter shares a common dc bus, which has been subdivided by six capacitors into seven levels. The voltage across each capacitor is  $V_{dc}/6$ , and the voltage stress across each switching device is limited to  $V_{dc}/6$  through the clamping diodes.  $m$ -level inverter leg requires  $(m - 1)$  capacitors,  $2(m - 1)$  switching devices and  $(m - 1)(m - 2)$  clamping diodes, by increasing the number of the output levels the total harmonic distortion will be reduced [7].



Table (3.1) lists the output voltage levels possible and their corresponding switch states for one phase of the inverter. State condition 1 means the switch is on, and State condition 0 means the switch is off. Each phase has six complementary switch pairs. For example when A1 turn on thus A1' must be turn off.

Table 3.1 Diode-clamped seven-level inverter voltage levels and corresponding switch states.

Voltage $V_{ao}$	Switch state											
	A1	A2	A3	A4	A5	A6	A1'	A2'	A3'	A4'	A5'	A6'
V7	1	1	1	1	1	1	0	0	0	0	0	0
V6	0	1	1	1	1	1	1	0	0	0	0	0
V5	0	0	1	1	1	1	1	1	0	0	0	0
V4V	0	0	0	1	1	1	1	1	1	0	0	0
V3	0	0	0	0	1	1	1	1	1	1	0	0
V2	0	0	0	0	0	1	1	1	1	1	1	0
V1	0	0	0	0	0	0	1	1	1	1	1	1

The steps to synthesize the seven-level voltages are as follows:

1. For an output voltage level  $V_{ao}=V_{dc}$ , turn on all upper-half switches A1, A2, A3, A4, A5 and A6.
2. For an output voltage level  $V_{ao}= 5V_{dc}/6$ , turn on upper switch A2, A, A4, A5, A6 and one lower switch A1'.
3. For an output voltage level  $V_{ao}= 4V_{dc}/6$ , turn on all lower half switches A3, A4, A5, A6 and A1', A2'.

4. For an output voltage level  $V_{ao} = V_{dc}/2$ , turn on all lower half switches, A4, A5, A6, and A1', A2', A3'.
5. For an output voltage level  $V_{ao} = V_{dc}/3$ , turn on all lower half switches, A5, A6, and A1', A2', A3', A4'.
6. For an output voltage level  $V_{ao} = V_{dc}/6$ , turn on all lower half switches, A6 and A1', A2', A3', A4', A5'.
7. For an output voltage level  $V_{ao} = 0$ , turn on all lower half switches, A1', A2', A3', A4', A5' and A6'.

The main advantages and disadvantages of multilevel diode-clamped converters are as follows:

Advantages:

- All of the phases share a common dc bus, which minimizes the capacitance requirements of the converter.
- The capacitors can be pre-charged as a group.
- Efficiency is high for fundamental frequency switching.

Disadvantages:

- It is becoming more difficult to control the power flow of the converter.
- The number of clamping diodes required is quadratically related to the number of levels, which can be cumbersome for units with a high number of levels.

### 3.3 Modulation Techniques

Various modulation techniques and control scheme have been developed for multilevel converters such as Multicarrier Pulse Width Modulation (PWM), selective harmonic elimination (SHE-PWM), space vector modulation (SVM), and others. Those techniques are shown in Fig 3.2. Here, only the level shifted multicarrier PWM techniques to control of the multilevel inverter is considered.

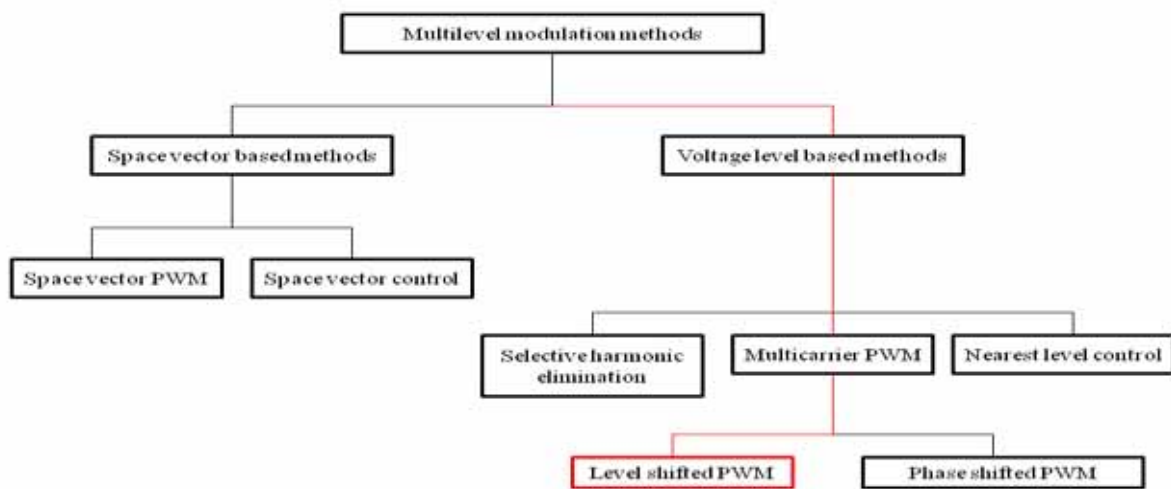


Fig 3.2 Modulation Techniques for multilevel inverter

To apply the multicarrier sinusoidal PWM (SPWM) method several triangular carrier signals with one modulating sinusoidal signal should be used to control multilevel inverter [7]. m-level inverter requires (m-1) triangular carrier signals. The carriers have the same frequency  $f_{cr}$  and the same peak to peak amplitude  $V_{cr}$ . The zero reference is placed in the middle of the carrier set. The modulating signal is a sinusoid of frequency  $f_m$  and amplitude  $V_m$ . The carrier signals are continuously compared with the modulating signal. If the modulating signal is greater than the triangular carrier the comparison gives 1, 0 otherwise. The results are added to give the voltage level, which is required at the output terminal of the inverter.

The frequency modulation index ( $mf$ ) is given by the relationship between the frequency of the Carrier frequency and the modulating signal as:

$$mf = f_{cr}/f_m \quad \dots\dots\dots (3.1)$$

The amplitude modulation index is given by:

$$ma = V_m/V_{cr}(m - 1) \quad \text{for, } 0 < ma < 1 \quad \dots\dots\dots (3.2)$$

There are three alternative strategies to implement level-shifted modulation [21]. They are as given below.

3.1 In-Phase Disposition (IPD), where all carrier waveforms are in phase as shown in Fig 3.3.

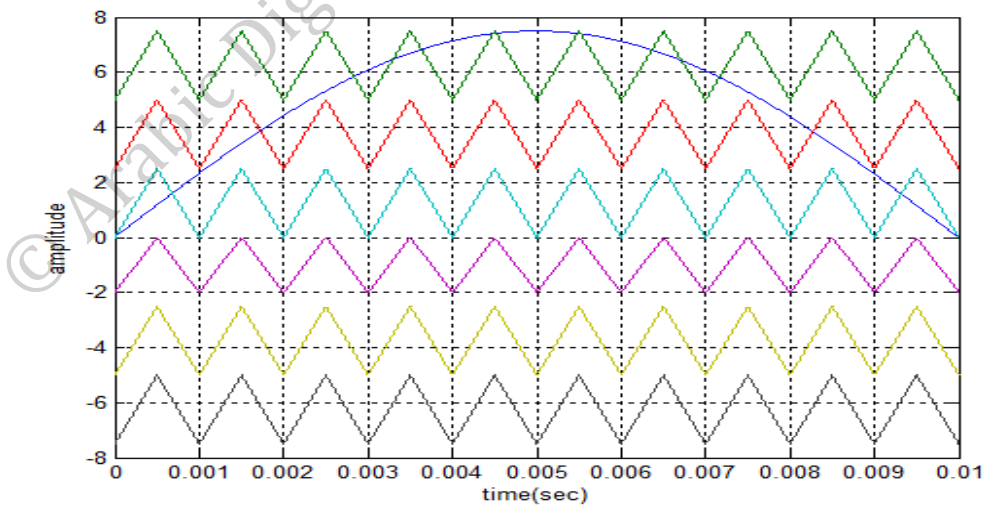


Fig 3.3 In-Phase Disposition (IPD)

3.2 Alternative Phase Opposite Disposition (APOD), where all carrier waveforms are alternatively in opposite disposition as shown in Fig 3.4.

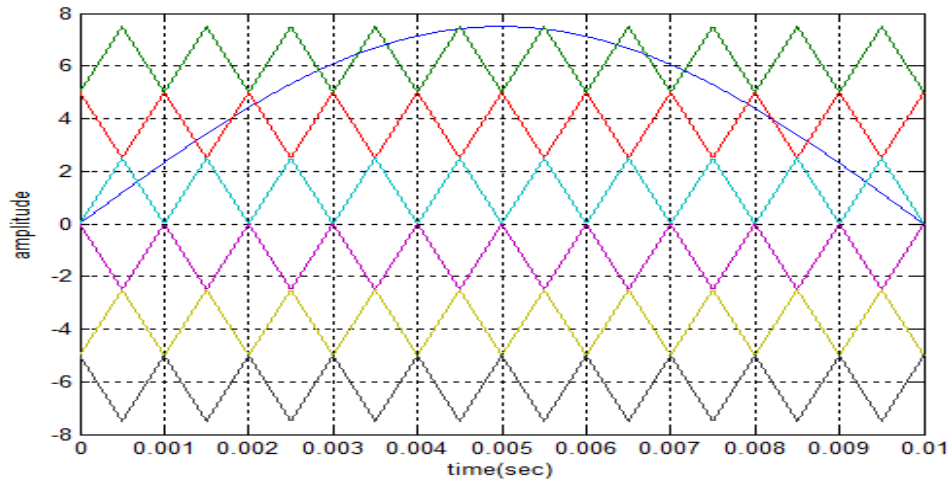


Fig 3.4 Alternative Phase Opposite Disposition (APOD)

3.3 Phase Opposite Disposition (POD), where all carrier waveforms above zero reference are in phase and are 180 degree out of phase with those below zero as shown in Fig 3.5.

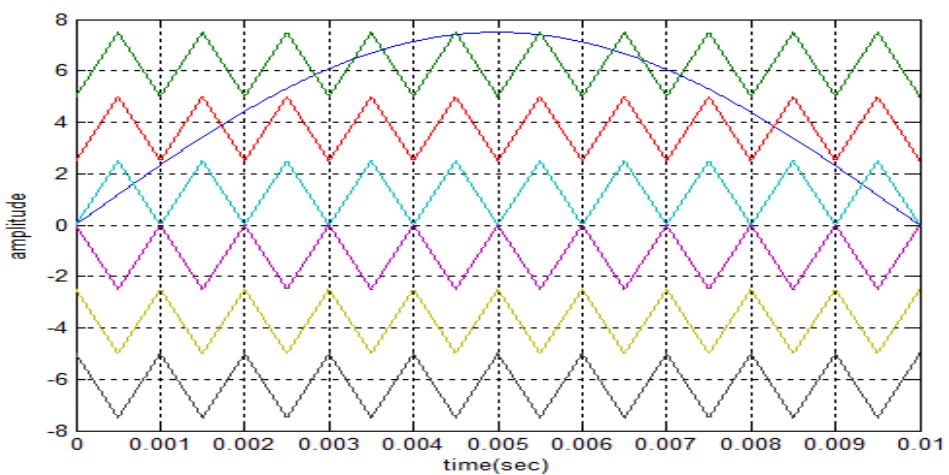


Fig 3.5 Phases Opposite Disposition (POD)

In general, the switching frequency of the inverter using the level-shifted modulation is given by:

$$f_{sw} = f_{cr} / (m - 1) \dots\dots\dots (3.4)$$

Where,

$f_{sw}$ : The switching frequency.

$m$ : number of level.

$f_{cr}$ : carrier frequency.

Fig 3.6 shows logic to generate gating signals for IGBTs in matlab simulink.

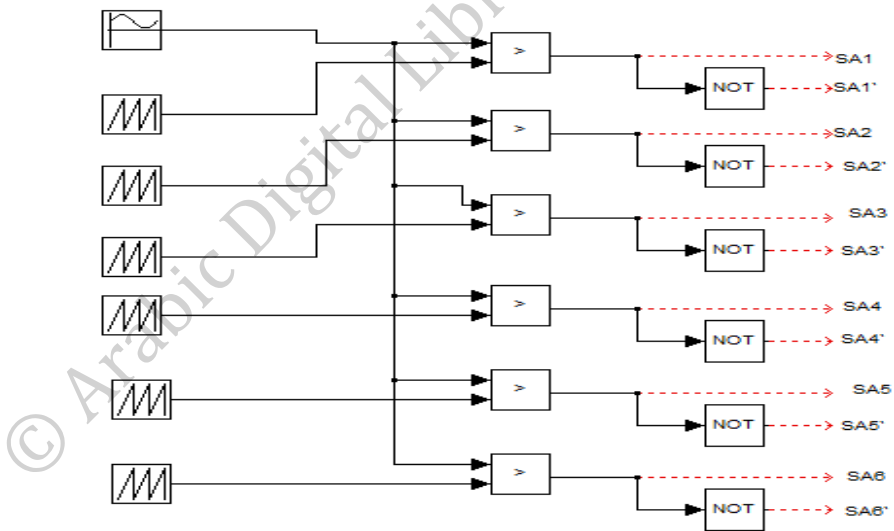


Fig 3.6 Logic to generate gating signals for IGBTs in Matlab Simulink.

### 3.4 Level Shifted Modulation Results

The three different schemes for the level shifted modulation have been simulated and compare them in order to evaluate the content of harmonics. The parameters used are shown in table 3.2.

Table 3.2 Parameters used for level shifted modulation technique

Frequency of the modulating signal wave ( $f_m$ )	50Hz
Peak amplitude of the modulating wave ( $V_m$ )	7.5
Frequency of the carrier wave ( $f_{cr}$ )	10kHz
Peak amplitude of the carrier wave ( $V_{cr}$ )	2.5
DC voltage	780

#### 3.4.1 In-phase disposition (IPD)

For the scheme based on phase disposition it has been found that the seven levels formed in the phase voltage and the thirteen levels formed in the line to line voltage as shown in Fig 3.7.

The harmonic spectrum for the output phase voltage and the line to line voltage obtained as shown in Fig 3.9 and Fig 3.10. The Total Harmonic Distortions (THD) obtained are 4.39% and 3.05% for the phase and line to line voltages respectively.

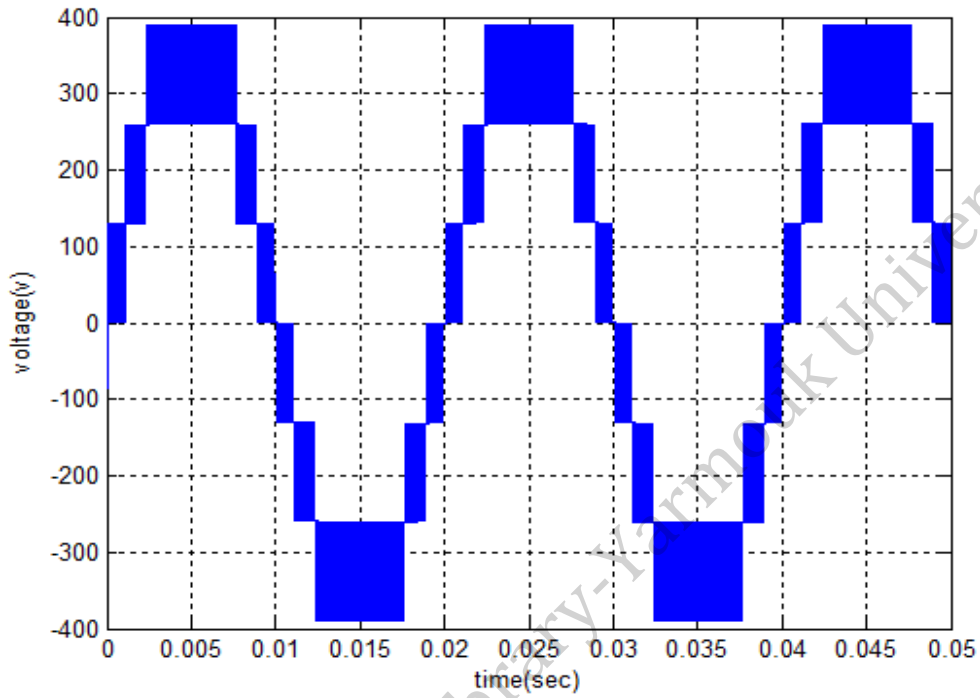


Fig 3.7 Output phase voltage

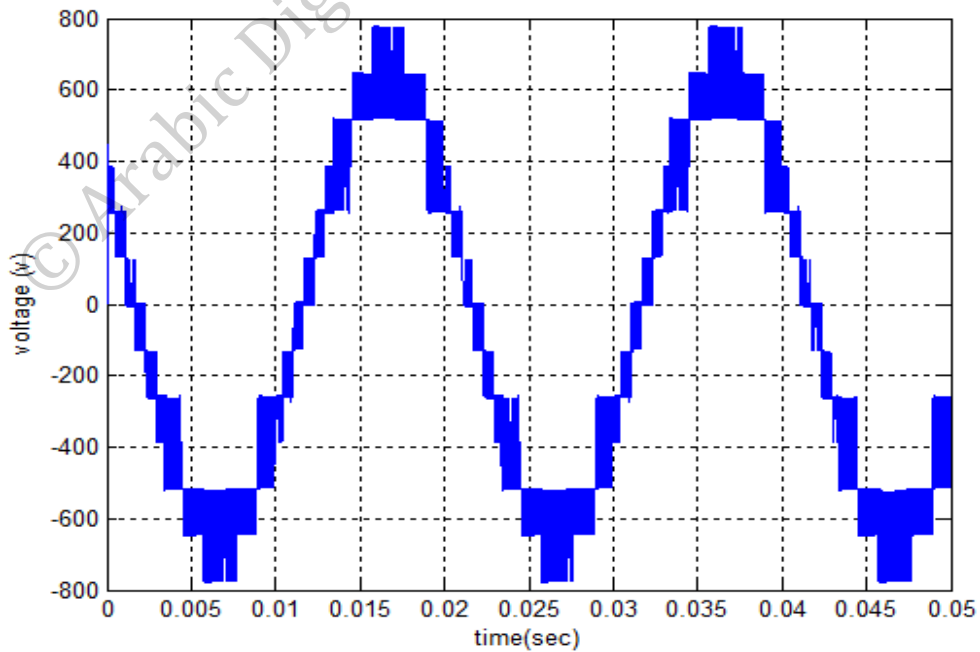


Fig 3.8 Output line to line voltage



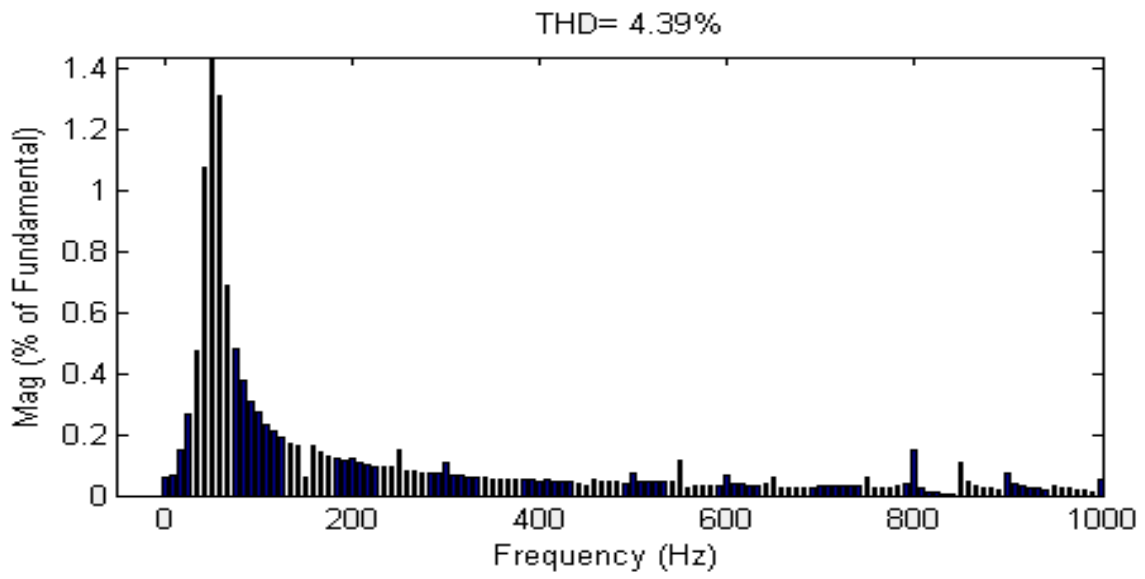


Fig 3.9 Harmonic Spectrum of phase voltage

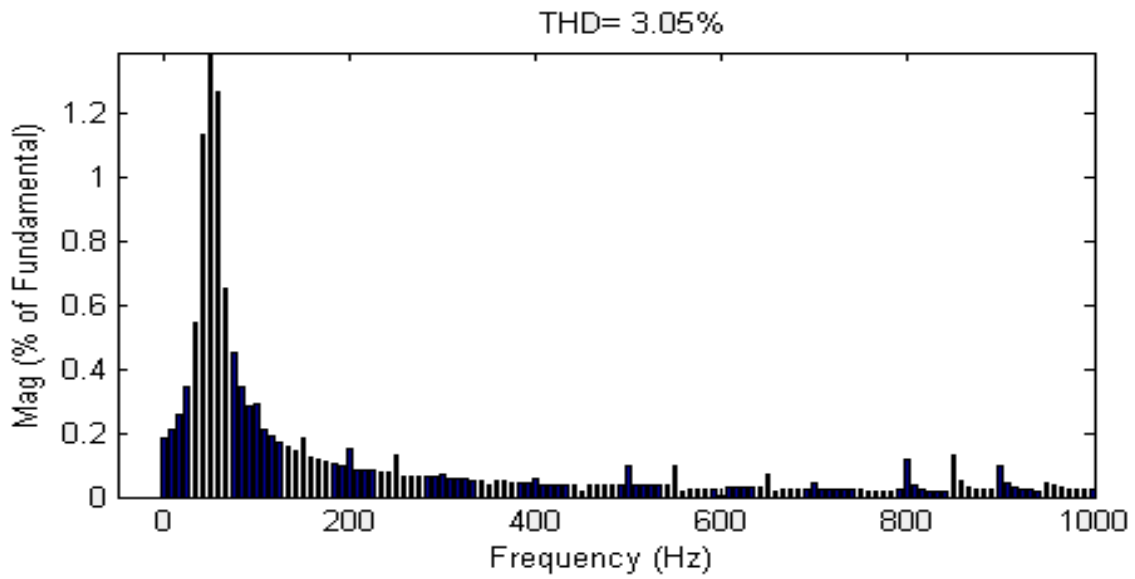


Fig 3.10 Harmonic Spectrum of line to line voltage

### 3.4.2 Alternative phase opposite disposition (APOD)

Based on alternative phase opposite disposition Fig 3.11 and Fig 3.12 show the THD values are 4.24% and 3.4% for the phase and line to line voltages respectively

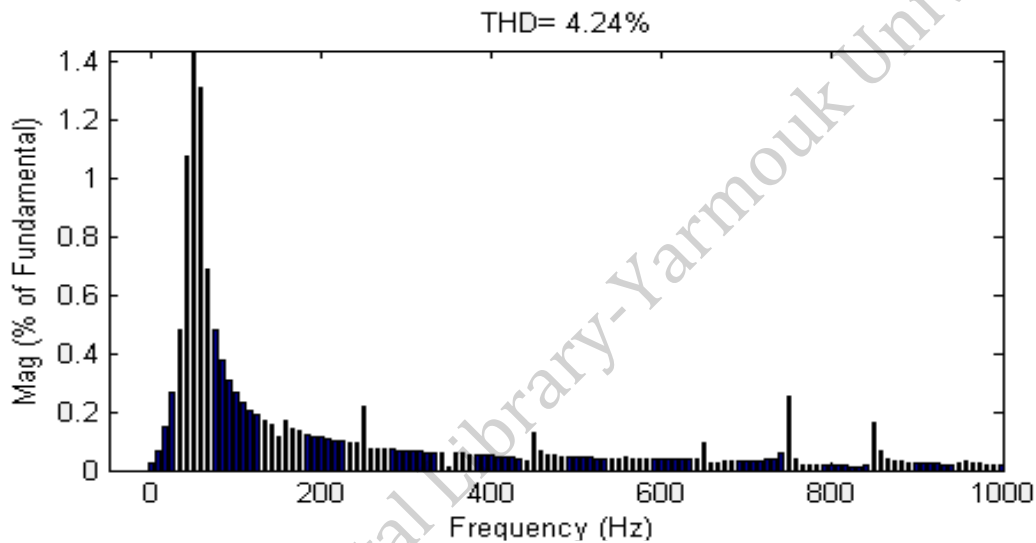


Fig 3.11 Harmonic Spectrum of phase voltage

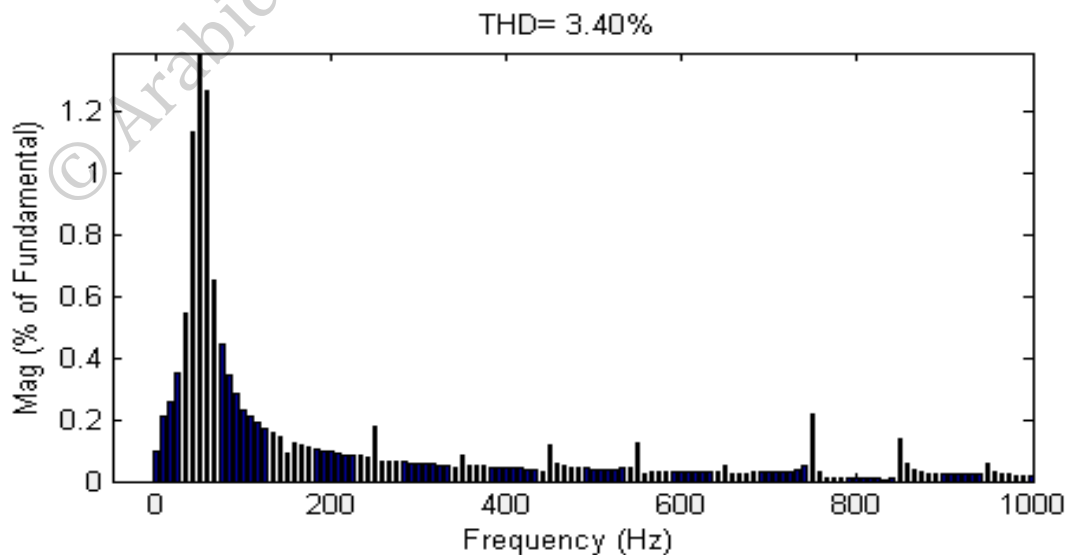


Fig 3.12 Harmonic Spectrum of line to line voltage

### 3.4.3 Phase opposite Disposition (POD)

For the scheme based on phase opposite disposition it has been found that the THD obtained are 4.40% and 3.57% for the phase and line to line voltages respectively as shown in Fig 3.13 and Fig 3.14.

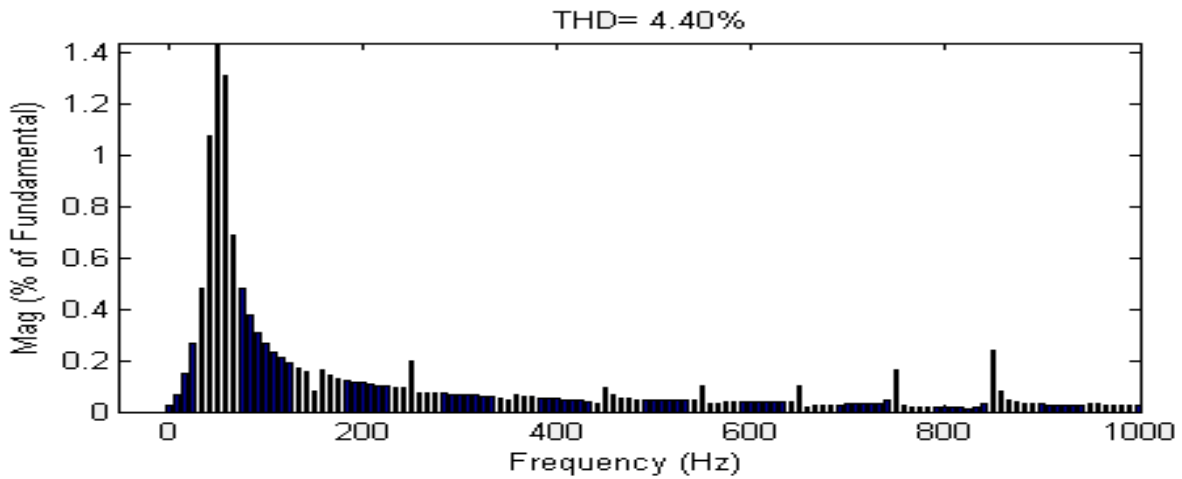


Fig 3.13 Harmonic Spectrum of phase voltage

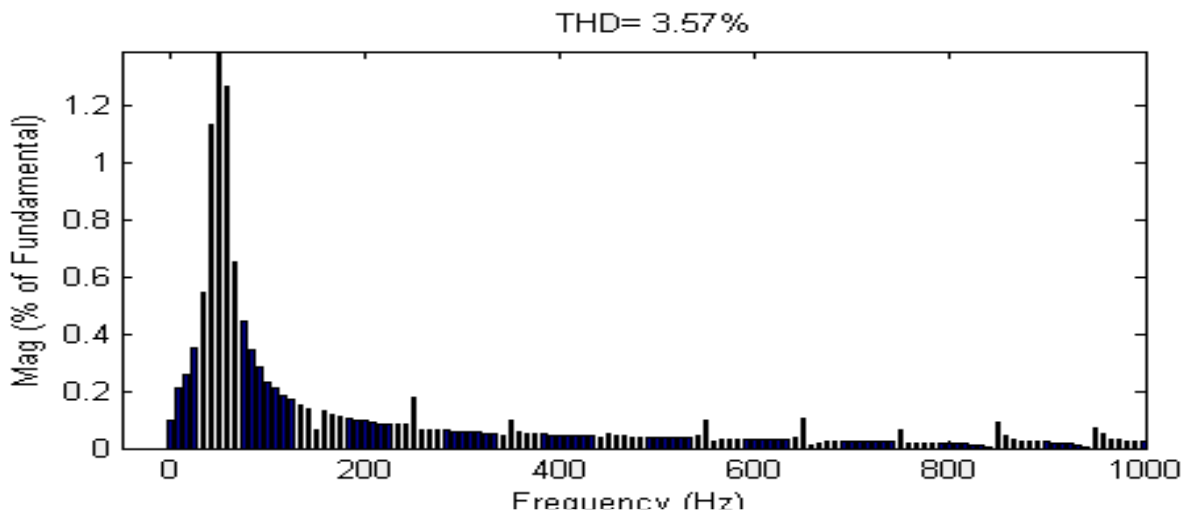


Fig 3.14 Harmonic Spectrum of line to line voltage

With base on the simulation results obtained in the figures above a comparison between the three schemes is presented in table 3.3. Table 3.3 shows the in phase disposition (IPD) presents the lowest THD of the line to line voltage, so the IPD Level shifted modulation scheme is chosen in this work as the modulation technique for the multilevel inverter.

Table 3.3 Level shifted modulation results

Level shifted modulation scheme	THD of line to line voltage	THD of phase voltage
In-phase disposition (IPD)	3.05%	4.39%
Alternative phase opposite(APOD)	3.4%	4.24%
Phase opposite Disposition (POD)	3.53%	4.40%

## Chapter 4: Dynamic modeling of induction motor

There are several models to describe the AC induction motor. The model used for vector control design can be obtained by using the space vector theory. The 3-phase motor quantities such as currents, voltages and flux are expressed in terms of complex space vectors. Such a model is valid for the analysis of transient and steady state performance of the induction motor [21]. This chapter focuses on Dynamic Model of the Induction Motor. The chapter starts with the three phase dynamic model of the induction motor, following by the Space Vector dynamic model of the induction motor in stationary reference frame ( $\alpha$ - $\beta$ ) and ending by the Space Vector dynamic model of the induction motor in rotating reference frame (d-q).

### 4.1 Three phase Mathematical modeling of induction motor

In order to analyze the induction machine, the following assumptions must be considered [22]:

- The induction motor is three-phase symmetrical
- The magnetic core is linear with a negligible core loss.
- The changing of parameters with temperature, are not considered.
- The flux density is radial in the air gape.
- The slotting effects are neglected.

A balanced three-phase machine is expressed in Figure 4.1 below.

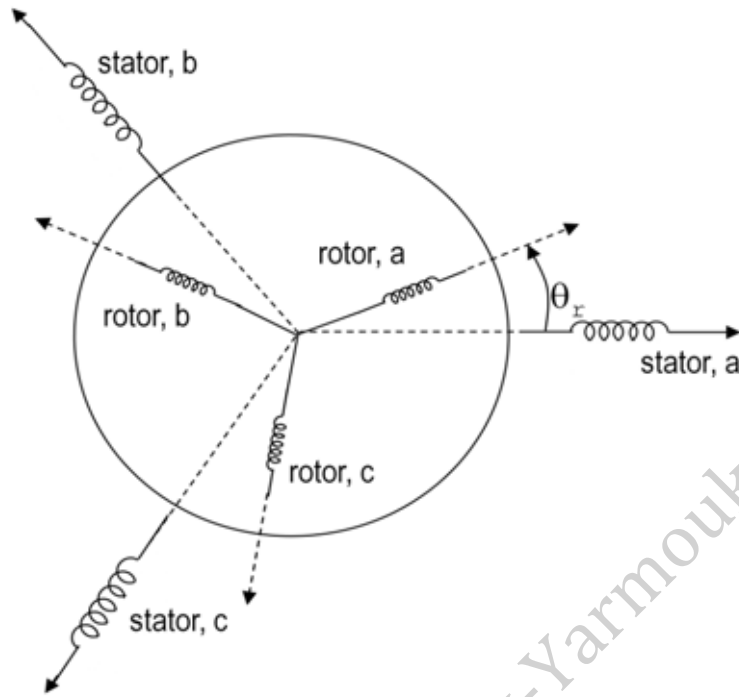


Fig 4.1 Equivalent Circuit of an AC induction motor

The stator and rotor voltages can be expressed as:

$$v_{abcs} = R_s i_{abcs} + d(\psi_{abcs})/dt \quad \dots\dots\dots (4.1)$$

$$v_{abcr} = R_r i_{abcr} + d(\psi_{abcr})/dt \quad \dots\dots\dots (4.2)$$

$$v_{abcs} = \begin{bmatrix} v_{as} \\ v_{bs} \\ v_{cs} \end{bmatrix} \quad i_{abcs} = \begin{bmatrix} i_{as} \\ i_{bs} \\ i_{cs} \end{bmatrix} \quad \Psi_{abcs} = \begin{bmatrix} \Psi_{as} \\ \Psi_{bs} \\ \Psi_{cs} \end{bmatrix} \quad \dots\dots\dots (4.3)$$

$$v_{abcr} = \begin{bmatrix} v_{ar} \\ v_{br} \\ v_{cr} \end{bmatrix} \quad i_{abcr} = \begin{bmatrix} i_{ar} \\ i_{br} \\ i_{cr} \end{bmatrix} \quad \Psi_{abcr} = \begin{bmatrix} \Psi_{ar} \\ \Psi_{br} \\ \Psi_{cr} \end{bmatrix} \quad \dots\dots\dots (4.4)$$

Where,

$v_{abcs}$ : the voltages applied to each stator phases

$v_{abcr}$ : are the voltages applied to each rotor phases .

$i_{abcs}$ : the currents in each stator phases

$i_{abcr}$ : the currents in each rotor phases .

$\psi_{abcs}$ : the fluxes linked with each stator phases

$\psi_{abcr}$ : the fluxes linked with each rotor phases.

$R_s$ : the stator resistance.

$R_r$ : the rotor resistance.

The flux in stator of the machine can be expressed with the flux created by the stator phases itself ( $\Psi_{abcs,s}$ ) and the flux part penetrating the stator originated from the rotor phases ( $\Psi_{abcs,r}$ ). In the same way the rotor flux can be expressed into the flux belonging to the rotor ( $\Psi_{abcr,r}$ ) and a part penetrating the rotor windings originating from the stator phases ( $\Psi_{abcr,s}$ ).

$$\Psi_{abcs} = \Psi_{abcs,s} + \Psi_{abcs,r} \dots\dots\dots (4.5)$$

$$\Psi_{abcr} = \Psi_{abcr,r} + \Psi_{abcr,s} \dots\dots\dots (4.6)$$

The flux can be expressed as a product of an inductance matrix and the current vector  $i$ .

The flux created from the stator windings is expressed as:

$$\Psi_{abc,s} = \begin{bmatrix} L_m + L_{ls} & -\frac{L_m}{2} & -\frac{L_m}{2} \\ -\frac{L_m}{2} & L_m + L_{ls} & -\frac{L_m}{2} \\ -\frac{L_m}{2} & -\frac{L_m}{2} & L_m + L_{ls} \end{bmatrix} \begin{bmatrix} i_{as} \\ i_{bs} \\ i_{cs} \end{bmatrix} \dots\dots\dots (4.7)$$

In the same way the flux created from the rotor windings can be expressed as:

$$\Psi_{abc,r} = \begin{bmatrix} L_m \left[ \frac{N_r}{N_s} \right]^2 + L_{lr} & -\frac{L_m}{2} \left[ \frac{N_r}{N_s} \right]^2 & -\frac{L_m}{2} \left[ \frac{N_r}{N_s} \right]^2 \\ -\frac{L_m}{2} \left[ \frac{N_r}{N_s} \right]^2 & L_m \left[ \frac{N_r}{N_s} \right]^2 + L_{lr} & -\frac{L_m}{2} \left[ \frac{N_r}{N_s} \right]^2 \\ -\frac{L_m}{2} \left[ \frac{N_r}{N_s} \right]^2 & -\frac{L_m}{2} \left[ \frac{N_r}{N_s} \right]^2 & L_m \left[ \frac{N_r}{N_s} \right]^2 + L_{lr} \end{bmatrix} \begin{bmatrix} i_{ar} \\ i_{br} \\ i_{cr} \end{bmatrix} \dots\dots\dots (4.8)$$

Where,

$L_m$ : the magnetizing inductance.

$L_{ls}$ : the stator leakage inductance.

$L_{lr}$ : the rotor leakage inductance.

The coupling between the rotor and stator is depending on the rotor displacement angle.

The flux penetrating the stator initiated in the rotor is shown in equation (4.9) and the stator flux penetrating the rotor is shown in equation (4.10).

$$\Psi_{abc,r} = \frac{N_r}{N_s} L_m \begin{bmatrix} \cos \theta_r & \cos(\theta_r + 2\pi/3) & \cos(\theta_r - 2\pi/3) \\ \cos(\theta_r - 2\pi/3) & \cos \theta_r & \cos(\theta_r + 2\pi/3) \\ \cos(\theta_r + 2\pi/3) & \cos(\theta_r - 2\pi/3) & \cos \theta_r \end{bmatrix} \begin{bmatrix} i_{ar} \\ i_{br} \\ i_{cr} \end{bmatrix} \dots\dots\dots (4.9)$$



$$\Psi_{abc,s} = \frac{N_r}{N_s} L_m \begin{bmatrix} \cos \theta_r & \cos(\theta_r - 2\pi/3) & \cos(\theta_r + 2\pi/3) \\ \cos(\theta_r + 2\pi/3) & \cos \theta_r & \cos(\theta_r - 2\pi/3) \\ \cos(\theta_r - 2\pi/3) & \cos(\theta_r + 2\pi/3) & \cos \theta_r \end{bmatrix} \begin{bmatrix} i_{as} \\ i_{bs} \\ i_{cs} \end{bmatrix} \dots\dots\dots (4.10)$$

Where,

$N_r$ : number of rotor turns windings.

$N_s$ : number of stator turns windings.

$\theta_r$ : the rotor displacement angle .

## 4.2 Space vector definition and projection

The three-phase stationary reference frame (a,b and c) variables such as voltages, currents and fluxes of AC-motors can be transformed into two-phase reference frame by using space vector theory [23]. Fig 4.2 shows the stator current complex space vector. Assuming that  $i_a, i_b, i_c$  are the instantaneous currents in the stator phases we can define the stator current vector  $i_s$  by:

$$i_s = k( i_{sa} + \alpha i_{sb} + \alpha^2 i_{sc} ) \dots\dots\dots(4.1)$$

Where,

$\alpha$ : represent the spatial operators and  $= e^{j2\pi/3}$ .

k: The transformation constant and is chosen 2/3.

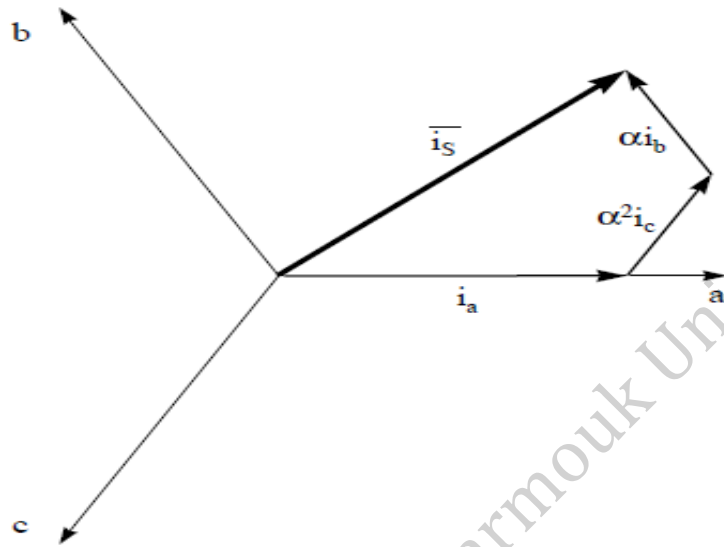


Fig 4.2 Stator Current Space Vector

#### 4.2.1 stationery reference frame ( $\alpha$ - $\beta$ )

Fig 4.2 shows stator current space vector projection in  $\alpha$ -  $\beta$  stationery reference frame. From Fig 4.2 the real part of the space vector is aligned to direct-axis stator current component,  $i_{s\alpha}$ , and the imaginary part is aligned to quadrature-axis stator current component,  $i_{s\beta}$ . Thus, three-phase stator current space vector can be expressed by two-phase stationery reference frame ( $\alpha$  and  $\beta$ ) as:

$$i_s = i_{s\alpha} + j i_{s\beta} \dots\dots\dots(4.2)$$

In symmetrical 3-phase machines, the stator current  $i_s$  can be resolved in to  $i_{s\alpha}$  and  $i_{s\beta}$  as follows:

$$i_{s\alpha} = k(i_{sa} - 0.5i_{sb} - 0.5i_{sc}) \dots\dots\dots (4.3)$$

$$i_{s\beta} = k\sqrt{3}/2 (i_{sb} - i_{sc}) \dots\dots\dots (4.4)$$

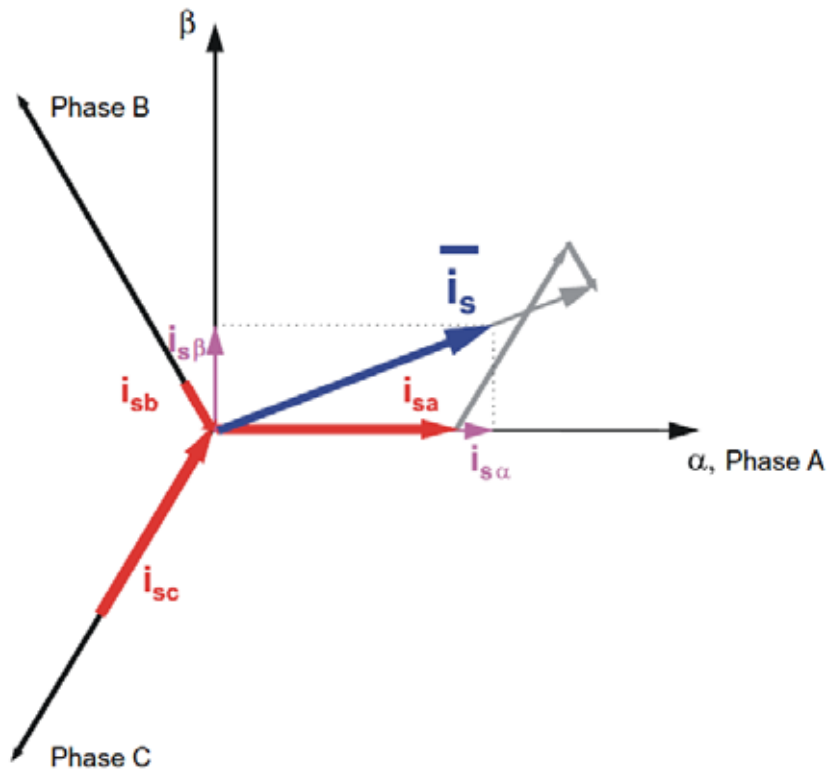


Fig 4.3 Stator current space vector and its projection

The space vectors of other motor quantities (voltages, currents, magnetic fluxes, etc.) can be defined in the same way as the stator current space vector.

The AC induction motor model is given by the space vector form of the voltage equations. The system model defined in the stationary ( $\alpha$ ,  $\beta$ ) coordinate system attached to the stator is expressed by the following equations:

- The stator voltage differential equations

$$v_{s\alpha} = R_s i_{s\alpha} + d(\psi_{s\alpha})/dt \quad \dots\dots\dots (4.5)$$

$$v_{s\beta} = R_s i_{s\beta} + d(\psi_{s\beta})/dt \quad \dots\dots\dots (4.6)$$

- The rotor voltage differential equations:

$$v_{r\alpha} = 0 = R_r i_{r\alpha} + d(\psi_{r\alpha})/dt + \omega_r \psi_{r\beta} \dots\dots\dots (4.7)$$

$$v_{r\beta} = 0 = R_r i_{r\beta} + d(\psi_{r\beta})/dt - \omega_r \psi_{r\alpha} \dots\dots\dots (4.8)$$

- The stator and rotor flux linkages expressed in terms of the stator and rotor current space vectors:

$$\left. \begin{aligned} \Psi_{s\alpha} &= L_s i_{s\alpha} + L_m i_{r\alpha} \\ \Psi_{s\beta} &= L_s i_{s\beta} + L_m i_{r\beta} \\ \Psi_{r\alpha} &= L_r i_{r\alpha} + L_m i_{s\alpha} \\ \Psi_{r\beta} &= L_r i_{r\beta} + L_m i_{s\beta} \end{aligned} \right\} \dots\dots\dots (4.9)$$

- Electromagnetic torque expressed by utilizing space vector quantities:

$$T_e = 3p/2 (\Psi_{s\alpha} i_{s\beta} - \Psi_{s\beta} i_{s\alpha}) \dots\dots\dots (4.10)$$

Where,

$L_s = L_{ls} + L_m$  represents the stator self-inductance.

$L_r = L_{lr} + L_m$  represents rotor self-inductance.

$T_e$ : electromagnetic torque.

$\omega_r$ : Electrical rotor speed.

### 4.2.2 Rotating reference frame (d-q)

Besides the stationary reference frame attached to the stator, the space-vector voltage equation can be expressed in a general reference frame rotates at an angular speed,  $\omega_g$ . Fig 4.4 shows two coordinate frame, x-y which rotating at a general instantaneous speed  $\omega_g = d\theta_g/dt$  and stationary reference frame  $\alpha$ -  $\beta$ . where  $\theta_g$  is the angle between the direct axis of the stationary reference frame ( $\alpha$ ) and the real axis (x) of the general reference frame, then the following equation defines the stator current space vector in general reference frame:

$$i_{sg} = i_s e^{-j\theta_g} = i_{sx} + j i_{sy} \quad \dots\dots\dots (4.11)$$

The stator voltage and flux-linkage space vectors can be similarly obtained in the general reference frame.

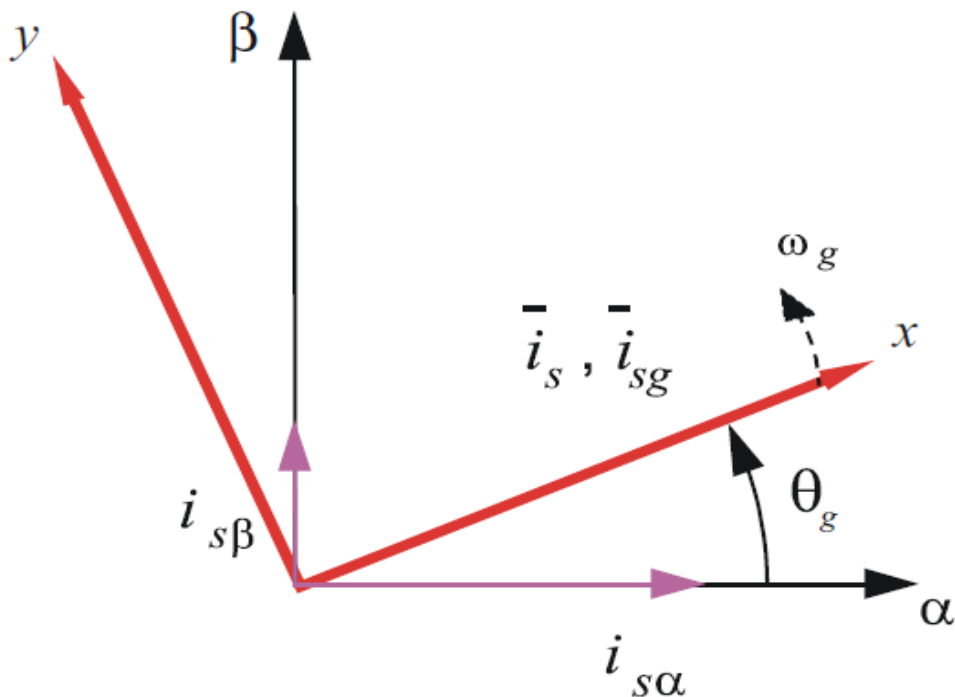


Fig 4.4 General reference frame rotates at a general speed  $\omega_g$ .

Similar considerations hold for the space vectors of the rotor voltages, currents and flux linkages. The real axis ( $r\alpha$ ) of the reference frame attached to the rotor is displaced from the direct axis of the stator reference frame by the rotor angle,  $\theta_r$ . As shown in Fig 4.4, the angle between the real axis ( $x$ ) of the general reference frame and the real axis of the reference frame rotating with the rotor ( $r\alpha$ ) is  $\theta_g - \theta_r$ . In the general reference frame, the space vector of the rotor currents can be expressed as:

$$i_{rg} = i_r e^{-j(\theta_g - \theta_r)} = i_{rx} + j i_{ry} \dots\dots\dots (4.12)$$

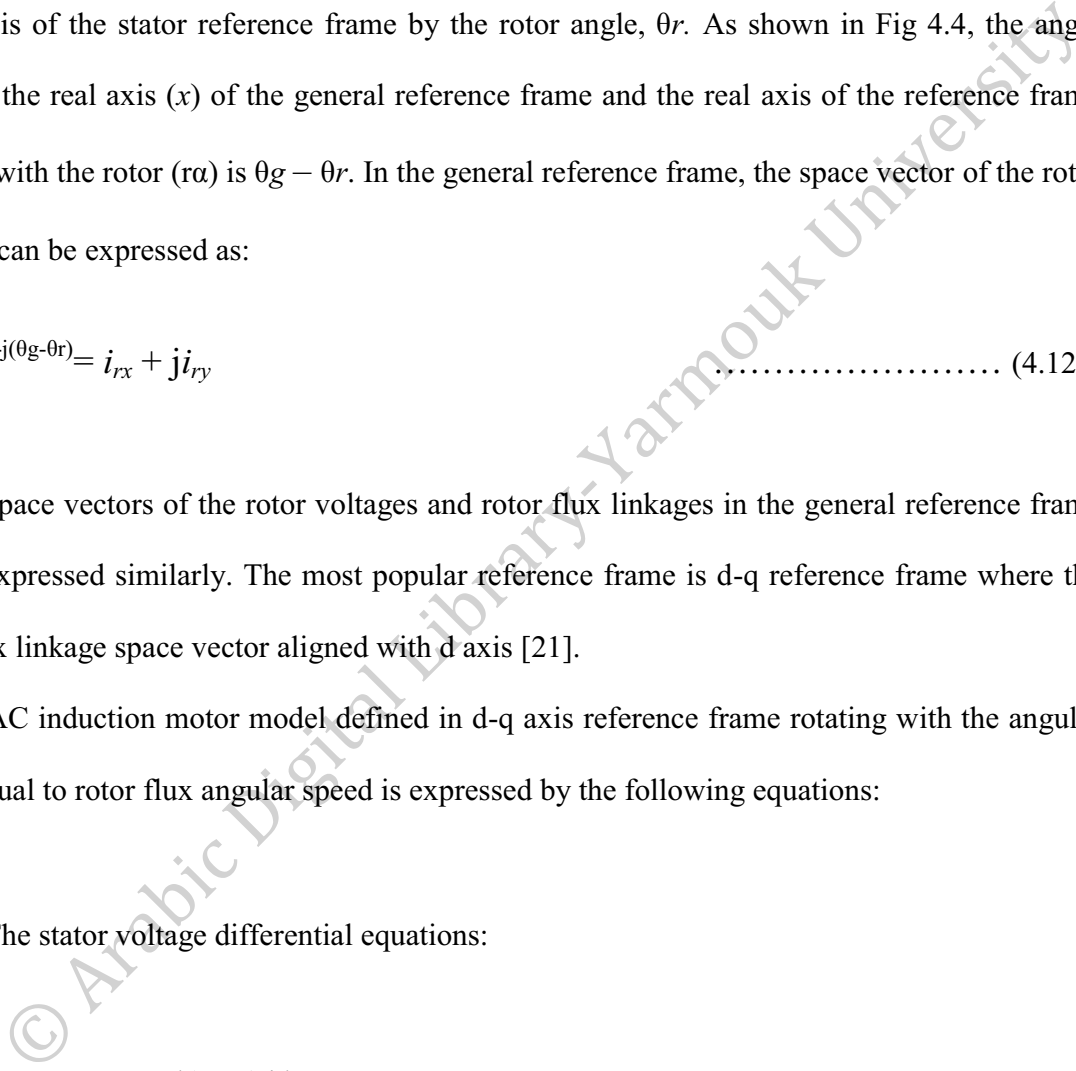
The space vectors of the rotor voltages and rotor flux linkages in the general reference frame can be expressed similarly. The most popular reference frame is d-q reference frame where the rotor flux linkage space vector aligned with d axis [21].

The AC induction motor model defined in d-q axis reference frame rotating with the angular speed equal to rotor flux angular speed is expressed by the following equations:

- The stator voltage differential equations:

$$v_{sd} = R_s i_{sd} + d(\psi_{sd})/dt - \omega_e \psi_{sq} \dots\dots\dots (4.13)$$

$$v_{sq} = R_s i_{sq} + d(\psi_{sq})/dt - \omega_e \psi_{sd} \dots\dots\dots (4.14)$$



- The rotor voltage differential equations:

$$v_{rd} = 0 = R_r i_{rd} + d(\psi_{rd})/dt - (\omega_e - \omega_r)\psi_{rq} \quad \dots\dots\dots (4.15)$$

$$v_{rq} = 0 = R_r i_{rq} + d(\psi_{rq})/dt + (\omega_e - \omega_r)\psi_{rd} \quad \dots\dots\dots (4.16)$$

The stator and rotor flux linkages expressed in terms of the stator and rotor current space vectors:

$$\left. \begin{aligned} \Psi_{sd} &= L_s i_{sd} + L_m i_{rd} \\ \Psi_{sq} &= L_s i_{sq} + L_m i_{rq} \\ \Psi_{rd} &= L_r i_{rd} + L_m i_{sd} \\ \Psi_{rq} &= L_r i_{rq} + L_m i_{sq} \end{aligned} \right\} \dots\dots\dots (4.17)$$

- Electromagnetic torque expressed by utilizing space vector quantities:

$$T_e = 3p/2 (\Psi_{sd} i_{sq} - \Psi_{sq} i_{sd}) \quad \dots\dots\dots (4.18)$$

Where,

$\omega_e$ : synchronous speed.

The representation of the above equations is shown below:

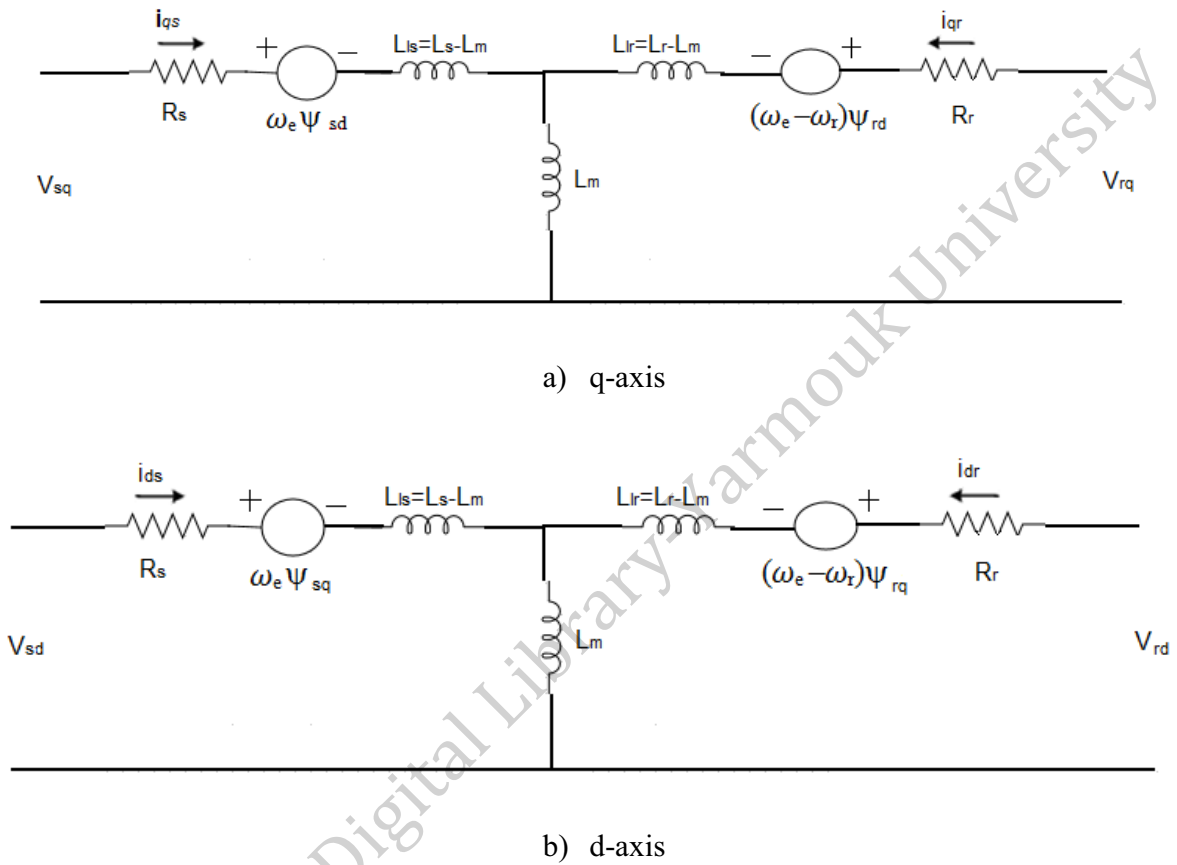


Fig 4.5 Dynamic d-q equivalent circuit (a) q-axis and (b) d-axis



## Chapter 5: Field Oriented Control and Simulation result

The concept of field oriented control is to achieve decoupled control over the torque and flux producing components of the stator currents like in separately excited dc machine [21] and [23]. To achieve this aim, a series of coordinate transformations, flux estimation and regulating will be done. This chapter focuses on FOC scheme for induction motor drives. The chapter starts with Principle of Operation of the vector control, follow by flux oriented control scheme based on PWM modulation and end by simulation results.

### 5.1 Concept of field oriented control

In a dc machine, neglecting the armature reaction effect and field saturation, the developed torque is given by [21]:

$$T_e = K_a i_a i_f \dots\dots\dots (5.1)$$

Where,

$K_a$ : armature constant.

$i_a$ : the armature current.

$i_f$ : the field current.

In the dc drive, the field flux  $\Psi_f$  produced by field current  $i_f$  and armature flux  $\Psi_a$  produced by armature current  $i_a$  are perpendicular. These space vectors, which are stationary in space, are orthogonal or decoupled in nature. It means that when torque is controlled by the current  $i_a$ , the flux  $\Psi_f$  is not changed because the decouple between  $\Psi_f$  and  $\Psi_a$  [21].

This technique can be applied to an AC induction motor if the machine is considered in synchronously rotating reference frame (d-q), where the variables appear as DC quantities in

steady state period. In general the vector control can be implemented in four different ways: rotor oriented, rotor flux oriented, stator flux oriented and magnetizing flux oriented. Here only the rotor flux oriented type, also known as FOC, is considered. Where the rotor flux vector  $\Psi_r$  is aligned to d-axis frame, which is rotating at synchronous speed with respect to stationary frame, as is shown in Figure 5.1

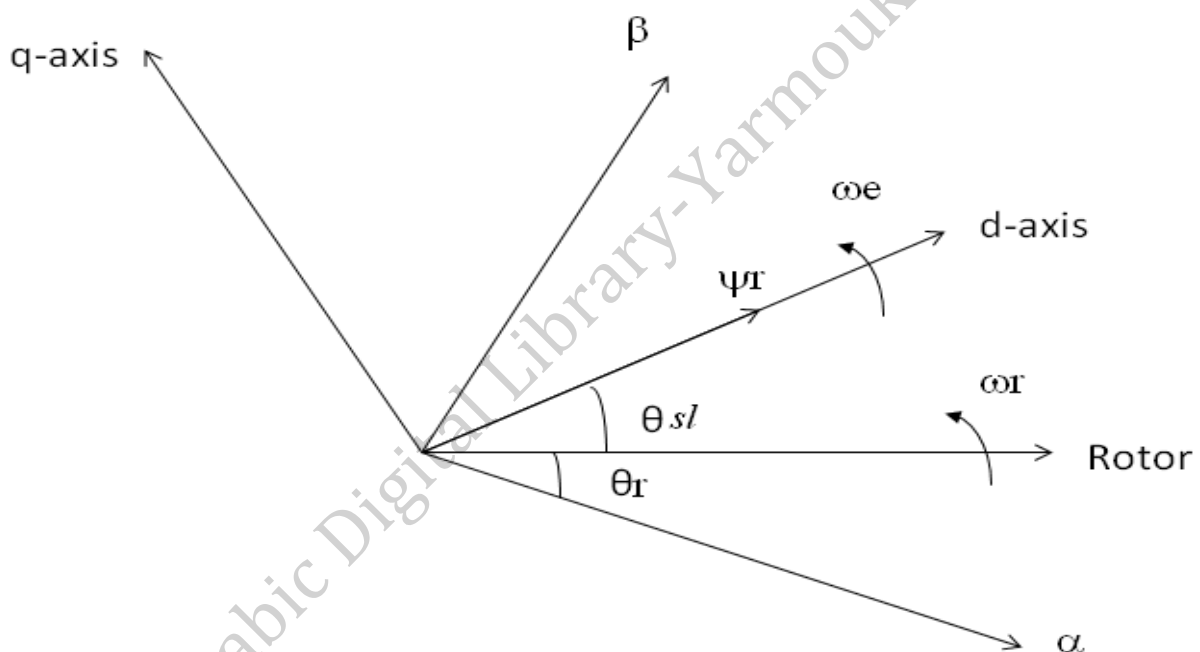


Fig 5.1 Rotor Flux Oriented Control.

## 5.2 Methods Based on FOC

Field orientation method can be classified into direct FOC (DFOC) and indirect FOC (IFOC) depending on the method used for rotor flux identification [24] and [25]. Where the rotor flux speed is not equal to the rotor speed (there is a slip speed) as shown in Fig 5.2. The DFOC is based on direct measuring of rotor flux vector by using flux sensor mounted in the air-gap. However, this strategy is not easy to implement because special modifications of the motor are

required for placing the flux sensors. The IFOC is based on measuring of rotor flux vector indirectly via slip calculations by using current and speed. In this work an indirect field oriented control has been used to control of IM fed by seven level diode clamped inverter.

### 5.2.1 Indirect field oriented control

An IFOC scheme for 7-level DCI fed IM drive is shown in Fig 5.2. In this strategy the rotor flux angle  $\theta_e$  is obtained from the measured rotor speed  $\omega_r$  and from the calculation of the slip speed  $\omega_{sl}$  as flow:

$$\theta_e = \int (\omega_r + \omega_{sl}) dt. \dots\dots\dots (5.2)$$

The slip speed  $\omega_{sl}$  is calculated from the stator reference current  $i_{qs}^*$  and the motor parameters as:

$$\omega_{sl} = \frac{Lm}{|\Psi_r|_{est}} \frac{Rr}{Lr} i_{qs}^* \dots\dots\dots (5.3)$$

The stator quadrature-axis current reference  $i_{qs}^*$  is calculated from torque reference  $T_e^*$  as:

$$i_{qs}^* = \frac{4}{3p} \frac{Lr}{Lm} \frac{T_e^*}{|\Psi_r|_{est}} \dots\dots\dots (5.4)$$

Where  $|\Psi_r|_{est}$  is the estimated rotor flux linkage given by:

$$|\Psi_r|_{est} = \frac{Lm \cdot i_{ds}}{1 + \tau_r \cdot s} \dots\dots\dots (5.5)$$

Where,

$\tau_r = Lr / Rr$  is the rotor time constant.

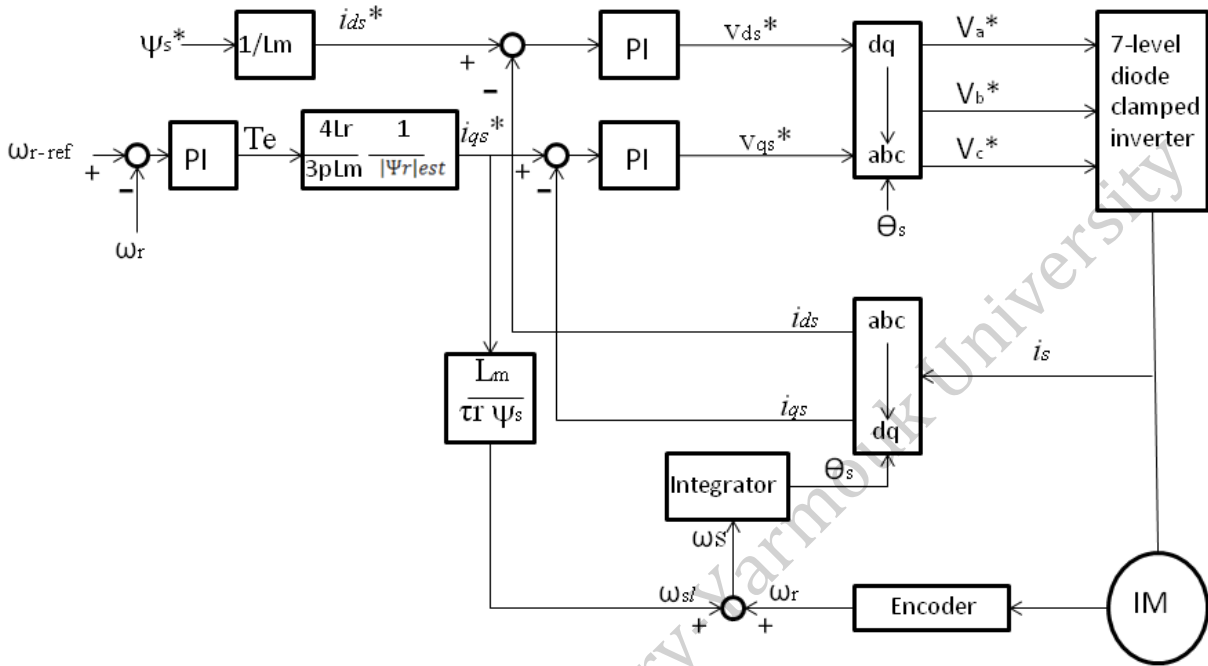


Fig 5.2 Indirect Field Oriented Control

The stator direct-axis current reference  $i_{ds}^*$  is obtained from rotor flux reference input  $|\psi_r|^*$ .

$$i_{ds}^* = \frac{|\psi_r|^*}{L_m} \dots \dots \dots (5.6)$$

### 5.2.2 Principle of operations

Firstly, the angular motor speed  $\omega_r$  has been measured by encoder connected to the motor shaft. Then the actual speed  $\omega_r$  has been compared with the reference speed  $\omega_{r-ref}$  and the error is processed by proportional-integral (PI) speed controller to produce a reference value of torque component. This value uses eq (5.4) to get the value of reference current  $i_q^*$ . The reference rotor flux is kept constant. Therefore, the flux producing component  $i_d^*$  is kept constant during operation as shown in eq (5.6). Then the reference current values ( $i_d^*$  and  $i_q^*$ ) are again processed individually by two inner loop current controller to generate reference voltage vectors

( $v_{ds}^*$  and  $v_{qs}^*$ ). These reference voltages are converted to three phase reference voltage vectors ( $v_a$ ,  $v_b$ , and  $v_c$ ). After that these reference voltages are used in multilevel inverter as a modulation signals to generate gate drive pulses for inverter.

### 5.3 Speed Loop Controller

A PI speed controller have been used in this work to keep the motor speed equal to the speed reference input in steady state and to provide a good dynamic during transient period. A trial and error method is used to find the proportional gain ( $K_p$ ) and integral gain ( $K_i$ ). The values selected for the speed loop PI controller are the proportional gain  $K_p = 15$  and the integral gain  $K_i = 55$ . A hysteresis band is used in the output of the speed control loop in order to limit the maximum electric torque developed during transient periods, this value is fixed in (-50, +50). The procedure to set up the controller parameters is shown in appendix A.

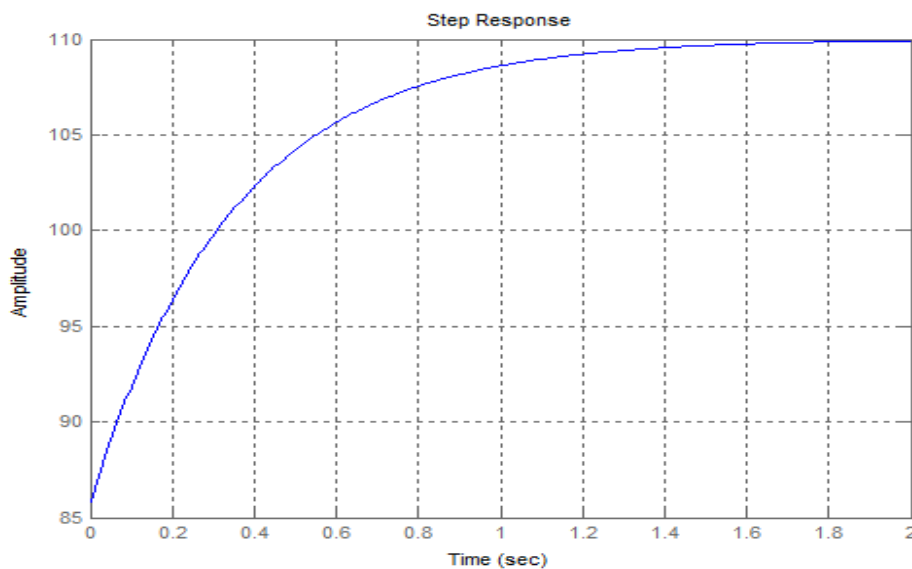


Figure 5.3 Step response of the speed controller.

## 5.4 Current Controllers

As is presented in section 5.2.2, field oriented control need two current controllers to control the current and generate the input references for the multilevel inverter. Several ways to implement those controllers [21] can be mentioned as:

- Hysteresis control.
- Stator frame PI controllers.
- Synchronous frame PI controllers.

### 5.4.1 Hysteresis Control

This method uses a hysteresis band to make the motor current tracks the reference current.

The following figure shows the operation principle of the hysteresis modulation [26].

The actual phase current compares with reference current. If current exceeds the upper limit of the hysteresis band, the upper switch of the inverter arm is turned off and the lower switch is turned on. As a result, the current starts to decay. If the current passes the lower limit of the hysteresis band, the lower switch of the inverter arm is turned off and the upper switch is turned on. As a result, the current gets back into the hysteresis band. Figure 5.5 details the hysteresis current control modulation scheme, consisting of three hysteresis comparators, one for each phase.

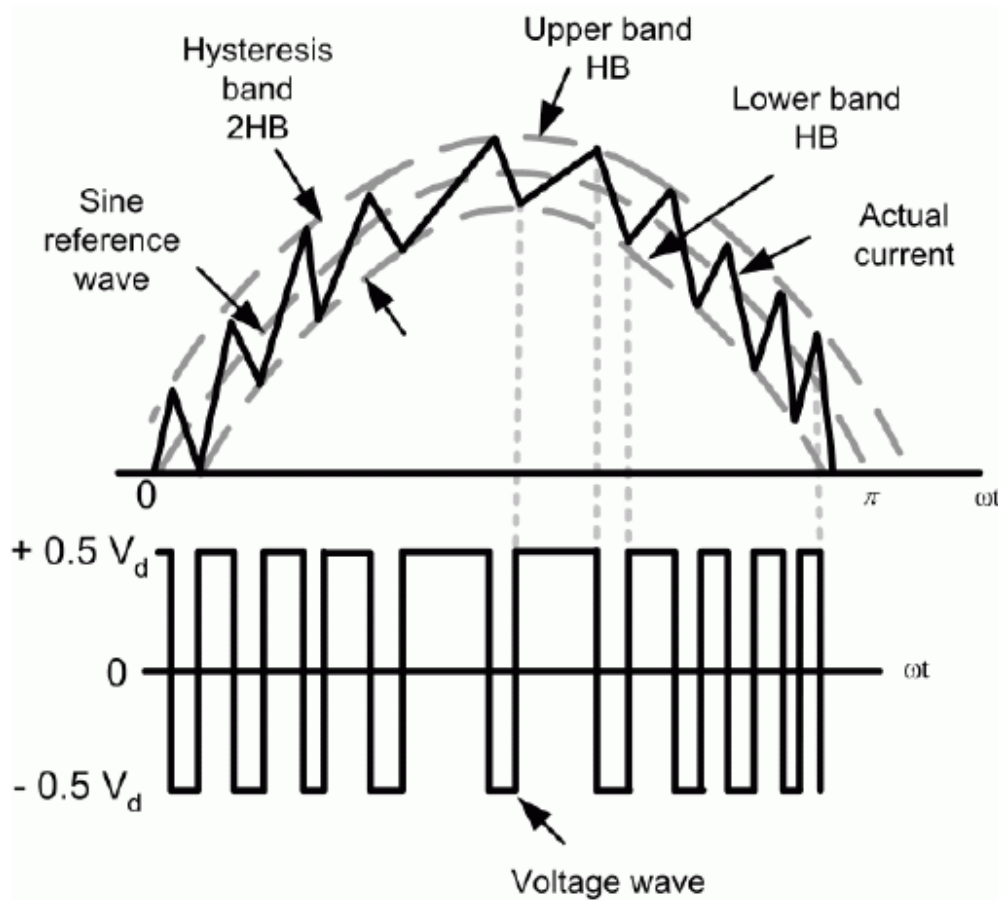


Fig 5.4 Principle of Hysteresis Control

One of the advantages of this control method is that pulse width modulation (PWM) is made directly by the controller. Therefore no additional circuit or algorithm is required. The difficulty of implementation in digital devices is one of the main drawbacks of this method.

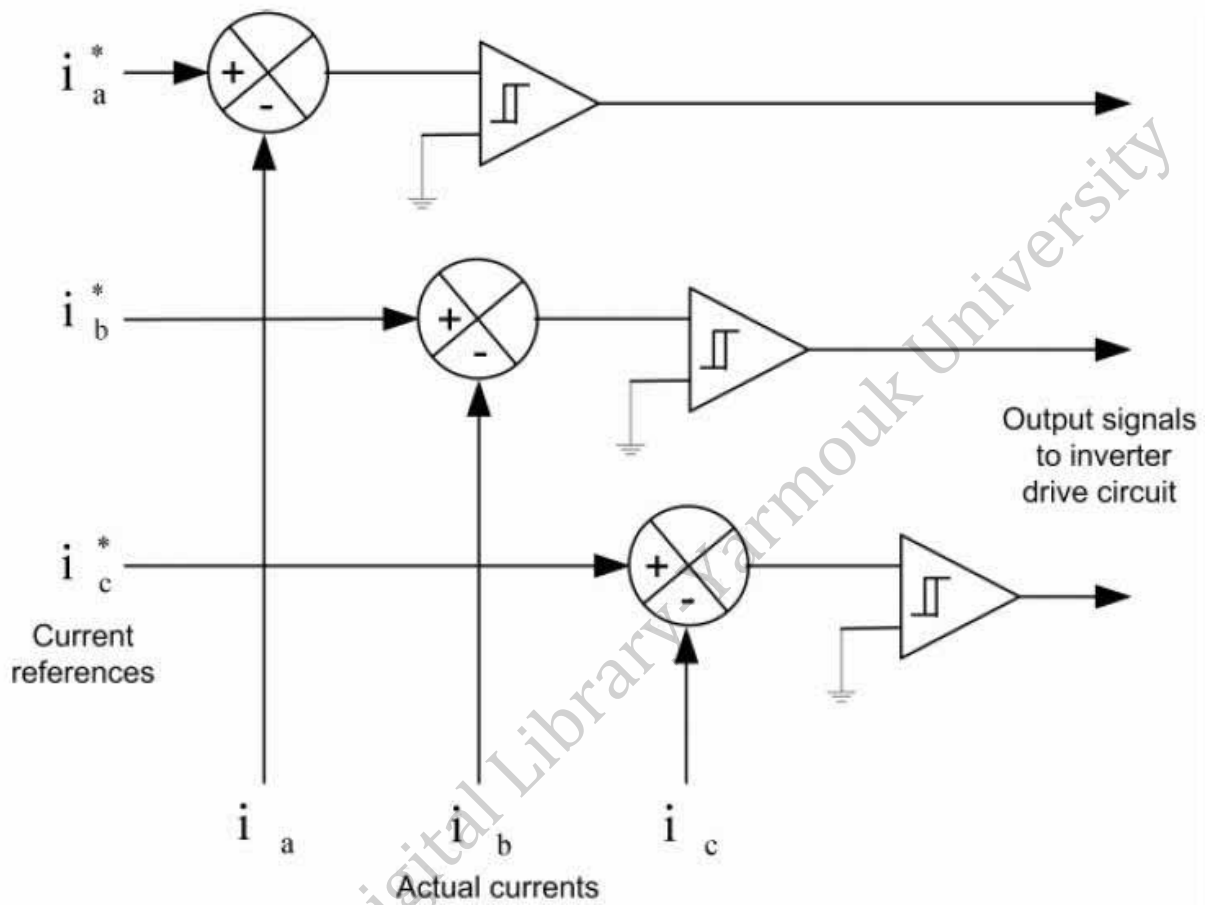


Fig 5.5 Scheme of Hysteresis Current Control

#### 5.4.2 Stator frame PI controllers

For this scheme is common to use two standard PI controllers (one each for the  $\alpha$  and  $\beta$  axes). The controller outputs are used as command signals to a PWM circuit. Unlike hysteresis control, this scheme uses two stages: control and modulation. One of the advantages of this scheme is that any PWM scheme can be employed. The drawback of this control scheme is that the actual current will not follow the reference in the steady state [2]. The control scheme is shown in figure 5.6.



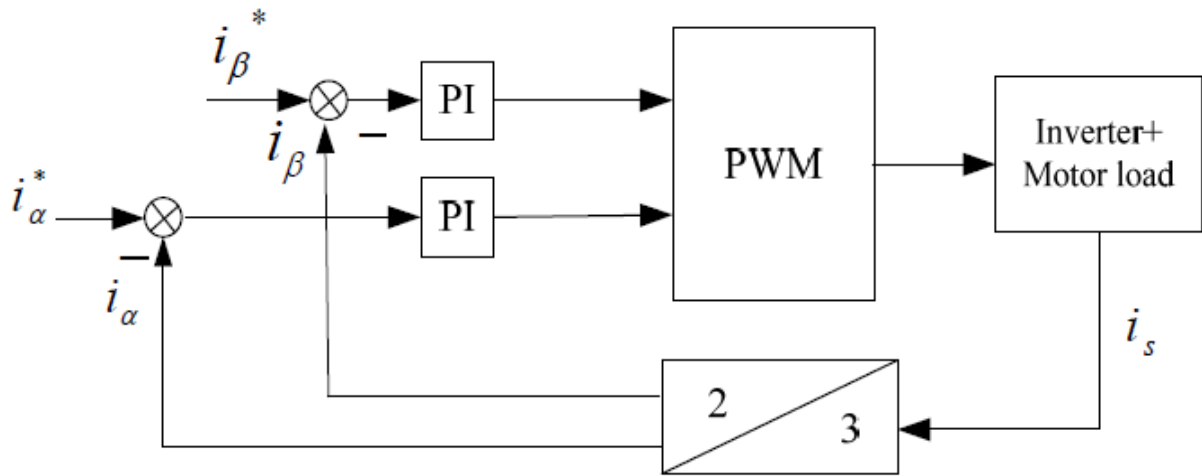


Fig 5.6 Stator Frame PI Controllers

### 5.4.3 Synchronous - Frame PI Control

In the synchronous frame PI control the  $\alpha\beta$  sinusoidal signals can be transformed to the synchronously rotating reference frame ( $dq$ ). The coordinate transformation requires some multiplications and the calculation of sine and cosine of the transformation angle.

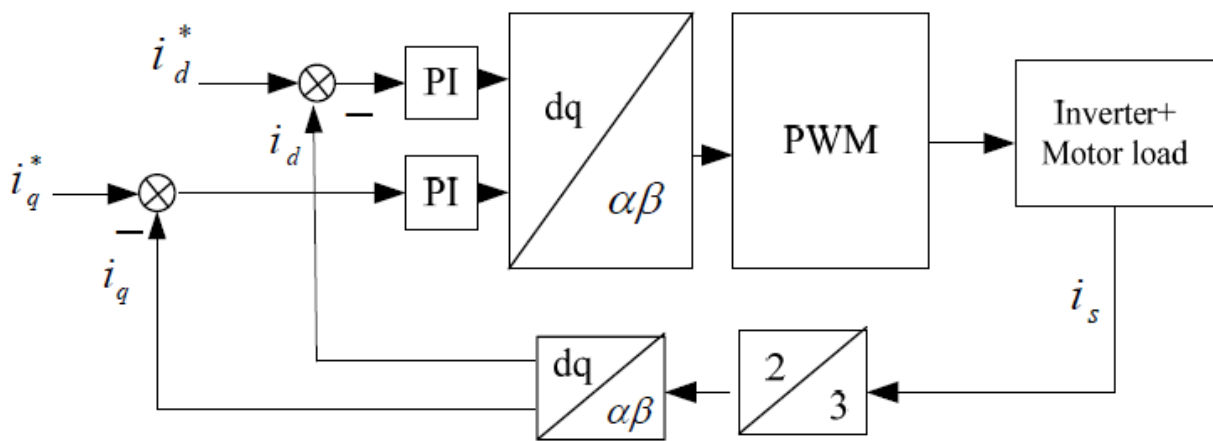


Fig 5.7 Synchronous - Frame PI Control

Synchronous-frame PI controllers is the most attractive choice for current control, due to their simplicity and ability to provide satisfactorily good performance. So the Synchronous - Frame PI Control is chosen in this work as the current controller. A trial and error method is used to find the proportional gain ( $K_p$ ) and integral gain ( $K_i$ ). The values selected for both Synchronous - Frame PI controller are the proportional gain  $K_p = 11$  and the integral gain  $K_i = 57$ .

### 5.5 Simulation Results

In order to investigate the performance of IFOC scheme for 7-level DCI fed IM drive, a detailed model has been developed in SIMULINK. Based on the above parameters the machine initially operates at zero speed and 0.7 as a reference flux. The machine accelerates under no-load conditions until the reference speed of 110 rad/s is reached at 0.4 sec as is shown in figure below.

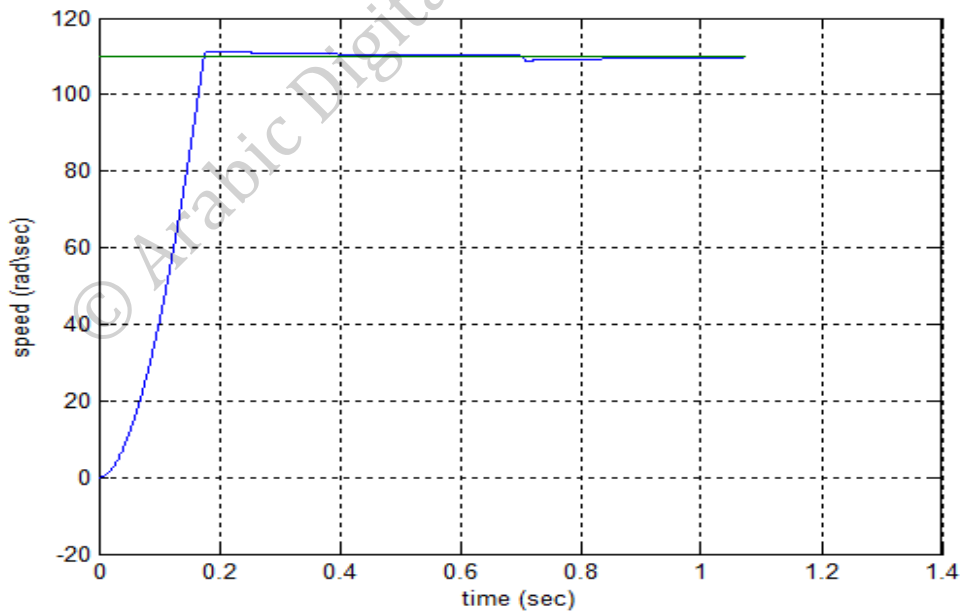


Fig 5.8 Speed response

A Load of 45Nm is connected to the machine at time instant of 0.7sec and the speed drops to 108.8 rad/sec. The controller takes 0.18 sec to restore the speed to the rated value as shown.

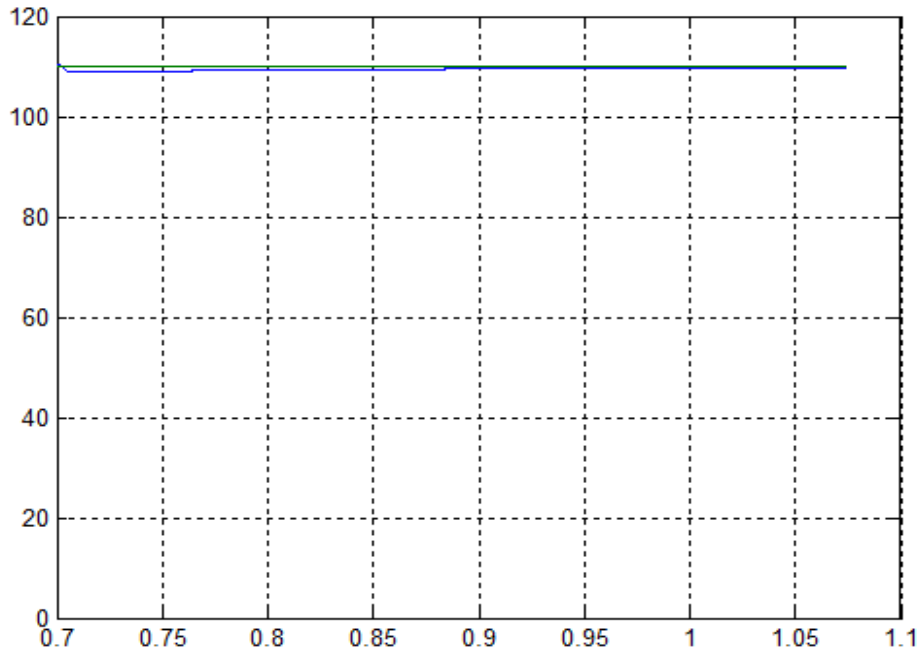


Fig 5.9 Speed variation at  $t=0.7$  s when a load of 45Nm is connected.

Fig 5.10 shows the variation of the electrical Torque which is increase until 55.8Nm during the transient period, and drop to zero during the steady state period. The torque contains ripple due to the switching frequency. The torque ripples up to  $\pm 1$ N.m.

Fig 5.11 shows the behavior of the stator currents during the transient and steady state periods. From figure 7 can be noted that during the transient period the current is increased until 31.5A. During the non load conditions of the machine, the current is remained in 20.35A. When the load is connected at 0.7 sec. the current achieves a value of 22.2A given by the new electrical torque.

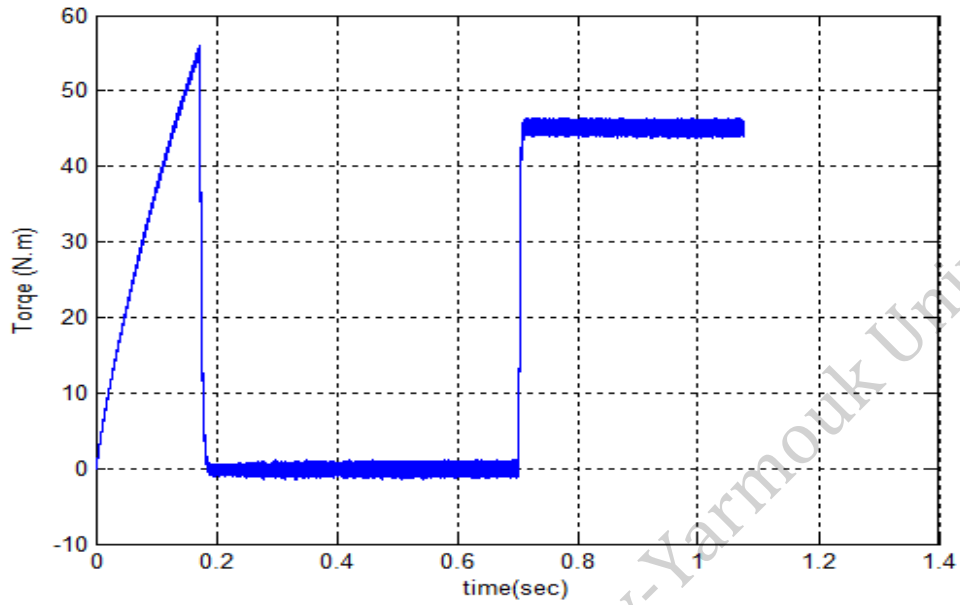


Fig 5.10 Torque response

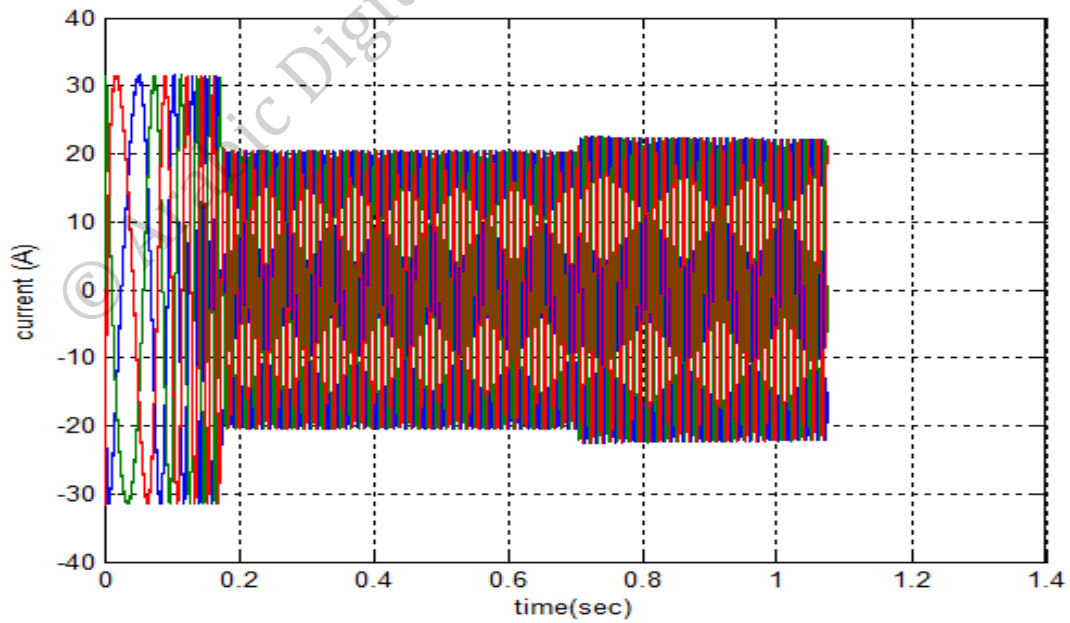


Fig 5.11 Three phase stator currents

The line-line voltage (seven levels) generated by the inverter is presented in Fig 5.12. During the transient period less than seven levels are generated, as soon as the steady state is achieved as is shown in Fig 5.13, the completed levels are formed.

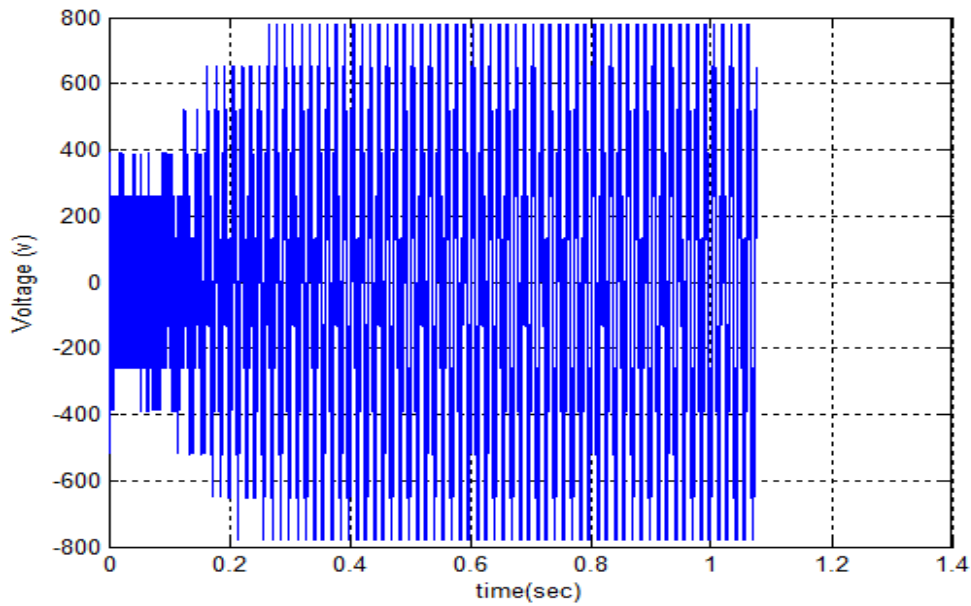


Fig 5.12 Line-Line voltage waveform

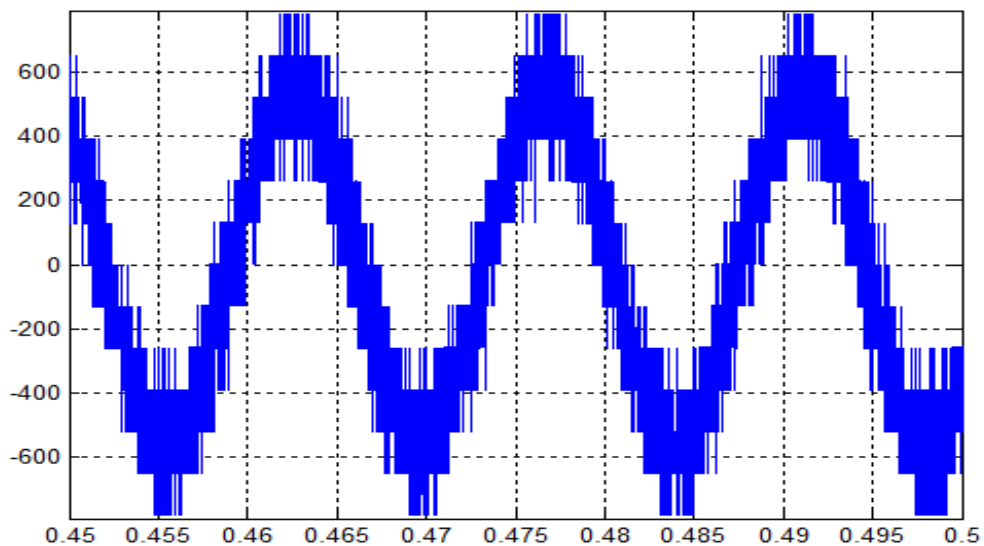


Fig 5.13 Line-Line voltage waveform in steady state

The inverter line-line voltage contains third harmonics as is shown in Fig 5.14 and the THD in steady state is 9.82%.

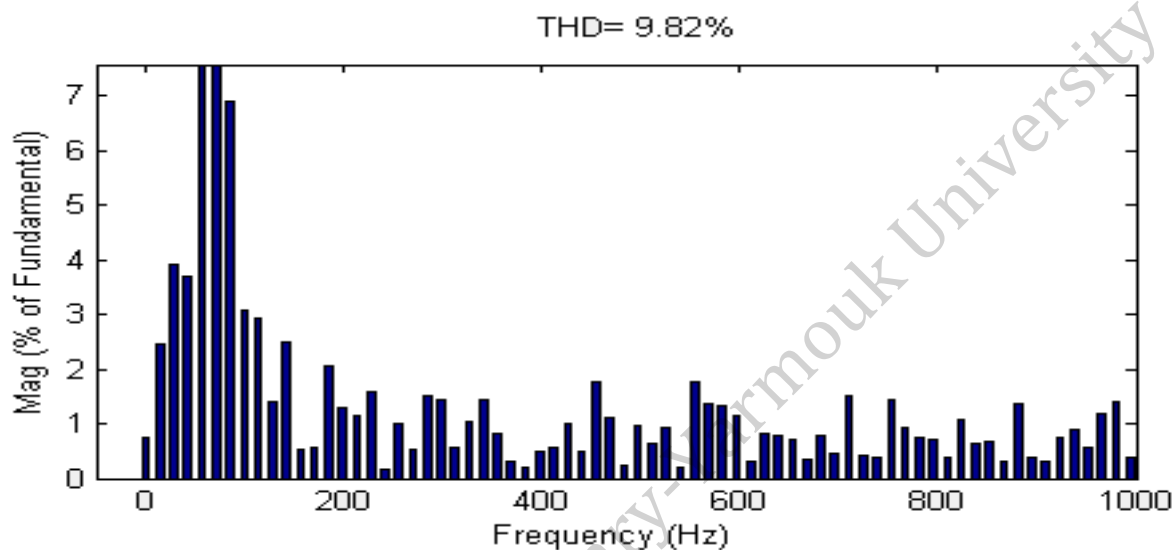


Fig 5.14 Harmonic Spectrum of line-line voltages of a phase A

The complete system operates again with different values of induction motor loads at time instant 0.7 sec. The simulation results are summarized in the table below.

Table 5.1 Response of the system with different values loads

load	Speed response(sec)	Current(ampere)	Torque ripple(N.M)
10	0.16	20.4	$\pm 1$
20	0.162	20.7	$\pm 1$
30	0.167	21.25	$\pm 1$
45	0.18	22.2	$\pm 1$
60	0.188	23.6	$\pm 1$
70	0.197	25	$\pm 1$

According to the table 5.1 the speed response and current increase when the connected load increase but the torque ripple does not change with different loads because the torque ripple depending on multilevel inverter.

## Chapter 6: conclusion and future work

### 6.1 Conclusion

In this thesis the indirect field oriented control for induction motor feed by 7-level diode clamped inverter was implemented using the MATLAB/SIMULINK software package. The level shifted carriers-base pulse width modulation (PWM) techniques were used to control of the multilevel inverter. According to the table 3.3 and simulation results, the In Phase Disposition (IPD) level shifted modulation presented the lowest total harmonic distortion (THD) of the line to line voltage. So the IPD Level shifted modulation scheme was chosen in this work as the modulation technique for the multilevel inverter.

The Indirect Field Oriented control scheme based on a Synchronous Frame proportional-integral (PI) current control and simulation results were presented in chapter five. The simulation results show that the system effectively controls the motor speed and successfully restore the speed when connected different load values, minimize torque ripple to  $\pm 1$  and enhances the drive performance through reduction in (THD) to 9.76%.



## 6.2 Future work

Future research work may be divided into three aspects:

1. The present work has been carried out for a small machine. It can be extended for typical rated values of drives in the industry, up 12MW.
2. The control methods should be developed for the other two topologies multilevel inverter; cascade H-bridge and flying capacitor (capacitor clamped) multilevel inverter.
3. The modulation technique can be developed by using space vector PWM.

## References:

- [1] Brian A. Welchko and Thomas A. Lipo, "A Novel Variable-Frequency Three-Phase Induction Motor Drive System Using Only Three Controlled Switches" IEEE transaction on industry applications, VOL. 37, NO. 6, NOVEMBER/DECEMBER 2001.
- [2] Baoming Ge, Fang Zheng Peng, Aníbal T. de Almeida and Haitham Abu-Rub, "An Effective Control Technique for Medium-Voltage High-Power Induction Motor Fed by Cascaded Neutral-Point-Clamped Inverter" IEEE transaction on industry applications, VOL. 57, NO. 8, AUGUST 2010.
- [3] Marcin Żelechowski "Space Vector Modulated – Direct Torque Controlled (DTC – SVM) Inverter – Fed Induction Motor Drive" Ph.D. Thesis, Warsaw University of Technology, Warsaw – Poland, 2005.
- [4] G. Pandian and S. Rama Reddy" Simulation and analysis of multilevel inverter fed induction motor drive" Indian Journal of Science and Technology, Vol.2 No 2, Feb. 2009.
- [5] Ismail Khalil Bousserhane, Abdeldjabbar Hazzab, Mostefa Rahli, Mokhtar Kamliand Benyounes Mazari "Direct field oriented control using backstepping strategy with fuzzy rotor resistance estimator for induction motor speed control" ISSN 1392 – 124X INFORMATION TECHNOLOGY AND CONTROL, Vol.35, No.4, 2006.

- [6] Dr. Keith Corzine “Operation and Design of Multilevel Inverters” University of Missouri – Rolla, 2005.
- [7] Mr.S.Ebanezar Pravin andMs.R.Narciss Starbell” Induction Motor Drive Using Seven Level Multilevel Inverter for Energy Saving in Variable Torque Load Application” International Conference on Computer, Communication and Electrical Technology – ICC CET, 18th & 19th March, 2011.
- [8] Marcello Montanari, Sergei Peresada and Andrea Tilli” Aspeed-sensorless indirect field-oriented control for induction motors based on high gain speed estimation”sciencedirect, Automatica 42 1637 – 1650, (2006).
- [9] George A. Varsamis, Epaminontas D. Mitronikas and Athanasios N. Safacas” Field Oriented Control with Space Vector Modulation for Induction Machine Fed by Diode Clamped Three Level Inverter “IEEE International Conference on Electrical Machines, Paper ID 1084, 2008.
- [10] Beir Dandil and Servet Tuncer” four-quadrant control of multilevel inverter fed induction motor drives” journal of scientific and industrial research, VOL.67,pp688-696,septemper 2008.
- [11] Bimal k.Bose” modern power electronics and AC drives” the University of Tennessee, Knoxville, 2001, p.338.

- [12] Milan Zalman and Ivica Kuric” Direct Torque and Flux control of Induction machine and fuzzy controller” Journal of ELECTRICAL ENGINEERING, VOL. 56, NO. 9-10, 2005, 278–280.
- [13] Boonruang Marungsri, Nittaya Meeboov and Anant Oonsivila” Dynamic Model Identification of Induction Motors using Intelligent Search Techniques with taking Core Loss into Account” Proceedings of the 6th WSEAS International Conference on Power Systems, Lisbon, Portugal, September 22-24, 2006.
- [14] Ridwan Gunawan, Feri Yusivar and Zuhail A. Kadir” Field Oriented Control of An Induction Motor Speed Sensorless with Current Vector Controller , direct-quadrature Current Compensator and Full Order Observer In direct-quadrature Axis” The 2nd Indonesian Japan Joint Scientific Symposium 2006.
- [15] Stephen J. Chapman” Electrical machinery fundamentals” 4<sup>th</sup> edition 2005, BAE systems Australia, p 385.
- [16] Ville Naumanen” Multilevel converter modulation: implementation and analysis” Acta Universitatis Lappeenrantaensis , Doctor Thesis, the 7th of June, 2010.
- [17] Mohammed El Gamal, Ahmed Lotfy and G. E. M. Ali “Firing Approach for Higher Levels of Diode Clamped Multi-Level Inverters” Proceedings of the 14th International Middle East Power Systems Conference (MEPCON’10), Cairo University, Egypt, December 19-21, 2010, Paper ID 115.

- [18] V. Naga Bhaskar Reddy, V. Narasimhulu and Dr. Ch. Sai Babu” Control of cascade multilevel inverter by using carrierbased PWM technique and implemented to induction motor drive” ICGST-ACSE Journal, Volume 10, Issue 1, December 2010.
- [19] Leon M. Tolbert and Thomas G. Habetler “Novel Multilevel Inverter Carrier-Based PWM Methods” IEEE IAS 1998 Annual Meeting, St. Louis, Missouri, October 10-15, 1998, pp. 1424-1431.
- [20] Nashiren F. Mailah, Senan M. Bashi, Ishak Aris and Norman Mariun” Neutral-Point-Clamped Multilevel Inverter Using Space Vector Modulation” European Journal of Scientific Research, ISSN 1450-216X Vol.28 No.1 (2009), pp.82-91.
- [21] Luis Carlos Giraldo Vasquez” Control of a Variable Speed Drive with a Multilevel Inverter for subsea Applications” Norwegian University of Science and Technology, Master thesis, 04. February 2010.
- [22] Group PED4-1037” High Speed Field Oriented Control” Master Thesis, Aalborg University, 03th June 2009.
- [23] Fadhil A. Hassan “Field Oriented Control For Three Phase Induction Motor Based On Full Neural Estimator And Controller’ Eng. & Tech. Journal, Vol.28, No.15, 2010.
- [24] Dr. Rami A. Mahir, Dr. ZiadM. Ahmed and Mr. Amjad J. H” Indirect Field Orientation Control of Induction Machine with Detuning Effect” Eng.&Tech.Vol.26.No.1,2008.
- [25] T. Benmiloud and A. Omari “New Robust Approach of Direct Field Oriented Control of Induction Motor” World Academy of Science, Engineering and Technology 64 2010.

- [26] Hydro-Québec” SimPowerSystems™ User’s Guide” COPYRIGHT 1998–2011 by Hydro-Québec and the MathWorks, Inc.
- [27] Hemant Joshi, P. N. Tekwani and Amar Hinduja” Implementation of five level inverter using reversing voltage topology: a competitive solution for high power IM drive applications” National pwer electronics conference 2010.
- [28] Mohammad Reza Derakhshanfar” Analysis of different topologies of multilevel inverters” Master of Science Thesis, Chalmers University of technology, Göteborg, Sweden, 2010.
- [29] “Motor protection principles” Available: [www.gedigitalenergy.com](http://www.gedigitalenergy.com).
- [30] “The Pros and Cons of Having a Motor Rewound” Available: [www.wisdompage.com](http://www.wisdompage.com).
- [31] “Three- phase alternating current motors” Available: [www.pacontrol.com](http://www.pacontrol.com).
- [32] Maurizio Cirrincione , Marcello Pucci, Gianpaolo Vitale "A Novel Direct Torque Control of an Induction Motor Drive with a Three-Level Inverter" Ieee 2003.
- [33] M. S. Merzoug, and F. Nacéri “Comparison of Field-Oriented Control and Direct Torque Control for Permanent Magnet Synchronous Motor (PMSM)” World Academy of Science, Engineering and Technology 45 2008.

## Appendix A. speed controller.

%Tunning PI controller of speed Indirect Field oriented control

clc

clear all

$R_s=0.294$ ; %Stator resistance

$R_r=0.156$ ; %Rotor resistance

$L_s=0.00139$ ; %Stator inductance

$L_r=0.00074$ ; %Rotor inductance

$L_m=0.041$ ; %Magnetizing inductance

$L_R=L_r+L_m$ ;

$R=R_s+R_r$ ;

$L=L_s+L_r$ ;

$T_r=(L_r+L_m)/R_r$ ; % Time constant of Rotor

$I_d=15.8$ ;

$H=R_r/(L_R*I_d)$ ; %Plant transfer function

$K_p=15$ ; %Proportional gain of PI Controller

$T_i=0.2727$ ; %Time constant of PI Controller

$PI=K_p*(1+tf(1,[T_i 0]))$ ;

$A=PI*H$ ;

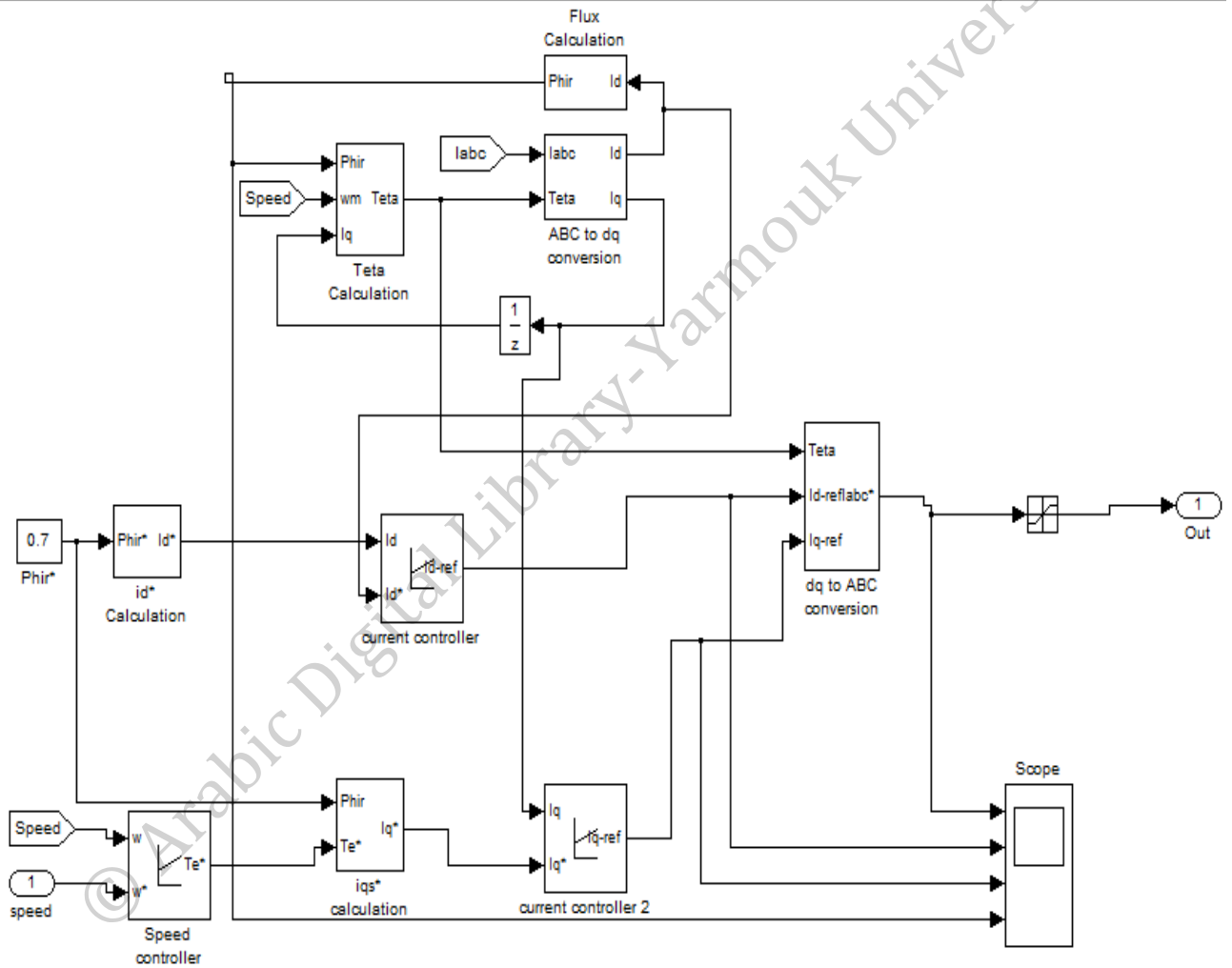
$R=A/(1+A)$ ;

$I_{ref}=110$ ;

step(R\*Iref,2)

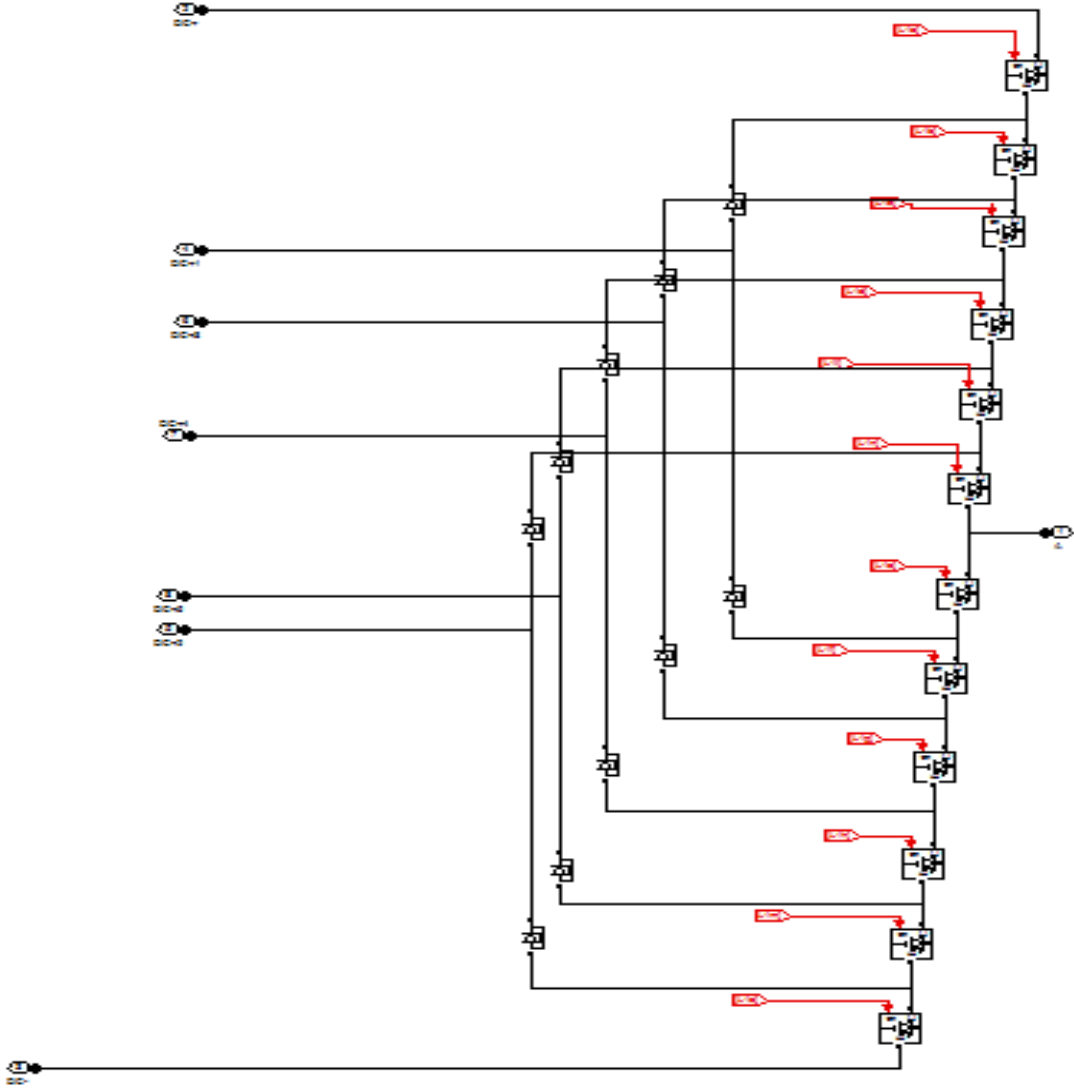
grid on

## Appendix B. Indirect Field Oriented Control Scheme in Matlab.





Appendix C. Leg A of Diode Clamped Inverter in Matlab



**Appendix D. Level shifted modulation in Matlab**

